

Genetic Architecture of Gene Expression in European and African Americans: An eQTL Mapping Study in GENOA

Lulu Shang,^{1,5} Jennifer A. Smith,^{2,5} Wei Zhao,² Minjung Kho,² Stephen T. Turner,³ Thomas H. Mosley,⁴ Sharon L.R. Kardia,^{2,*} and Xiang Zhou^{1,*}

Most existing expression quantitative trait locus (eQTL) mapping studies have been focused on individuals of European ancestry and are underrepresented in other populations including populations with African ancestry. Lack of large-scale well-powered eQTL mapping studies in populations with African ancestry can both impede the dissemination of eQTL mapping results that would otherwise benefit individuals with African ancestry and hinder the comparable analysis for understanding how gene regulation is shaped through evolution. We fill this critical knowledge gap by performing a large-scale in-depth eQTL mapping study on 1,032 African Americans (AA) and 801 European Americans (EA) in the GENOA cohort. We identified a total of 354,931 eSNPs in AA and 371,309 eSNPs in EA, with 112,316 eSNPs overlapped between the two. We found that eQTL harboring genes (eGenes) are enriched in metabolic pathways and tend to have higher SNP heritability compared to non-eGenes. We found that eGenes that are common in the two populations tend to be less conserved than eGenes that are unique to one population, which are less conserved than non-eGenes. Through conditional analysis, we found that eGenes in AA tend to harbor more independent eQTLs than eGenes in EA, suggesting potentially diverse genetic architecture underlying expression variation in the two populations. Finally, the large sample sizes in GENOA allow us to construct accurate expression prediction models in both AA and EA, facilitating powerful transcriptome-wide association studies. Overall, our results represent an important step toward revealing the genetic architecture underlying expression variation in African Americans.

Introduction

Genome-wide association studies (GWASs) have identified thousands of genetic variants that are associated with various diseases and disease-related complex traits. However, the vast majority of these disease-associated variants reside in non-coding regions and have unknown functions.^{1–4} While variants in non-coding regions cannot directly alter the function of a gene through disrupting protein-coding sequencing, they can influence the level of gene expression through impacting the regulatory mechanisms underlying expression. Indeed, in recent years, expression quantitative trait loci (eQTL) mapping studies have successfully identified many *cis*-acting genetic variants that are associated with gene expression levels.^{5–8} These identified eQTLs can help elucidate the molecular mechanisms underlying disease associations and facilitate the identification of biological pathways underlying disease etiology. For example, it has been shown that genetic variants associated with common diseases tend to be eQTLs and vice versa.^{1,9,10} In addition, identified eQTLs in mapping studies can also provide invaluable information to enhance the power of future GWASs.¹¹

To date, most existing eQTL mapping studies have been performed on individuals with European ancestry. eQTL mapping studies in other populations are noticeably underrepresented, with a particularly noticeable absence of

large studies in populations with African ancestry. Indeed, only a few eQTL mapping studies were carried out thus far on individuals with African ancestry and these studies often had small sample sizes that limited the statistical power of eQTL mapping. For example, HapMap3 included only 108 Yoruba (YRI) samples; the Geuvadis study included 89 YRI samples;¹² a study on population difference in immune response collected 100 individuals with African ancestry;¹³ and the Multi-Ethnic Study of Atherosclerosis (MESA) cohort included 233 African Americans.¹⁴ Because of differences in allele frequencies and linkage disequilibrium (LD) patterns, eQTL mapping results can vary, sometimes quite substantially, across populations with diverse genetic backgrounds.¹⁵ Consequently, eQTLs identified in one population are not necessarily eQTLs in another population, and eQTL mapping results from one population may not necessarily benefit or transfer to another population. In addition, and equally importantly, a lack of eQTL mapping studies in populations with African ancestry also hinders the progress of comparative analysis between Africans and other populations in terms of the genetic architecture differences underlying gene expression variation. Indeed, only a limited number of comparative studies have been performed between populations, and again with small sample sizes.^{12,16,17} Comparative studies on the genetic regulation of gene expression across populations can provide important insights into the genetic differences among populations that may

¹Department of Biostatistics, School of Public Health, University of Michigan, Ann Arbor, MI 48109, USA; ²Department of Epidemiology, School of Public Health, University of Michigan, Ann Arbor, MI 48109, USA; ³Division of Nephrology and Hypertension, Mayo Clinic, Rochester, MN 55905, USA; ⁴Memory Impairment and Neurodegenerative Dementia (MIND) Center, University of Mississippi Medical Center, Jackson, MS 39126, USA

⁵These authors contributed equally to this work

*Correspondence: skardia@umich.edu (S.L.R.K.), xzhousph@umich.edu (X.Z.)

<https://doi.org/10.1016/j.ajhg.2020.03.002>

© 2020 American Society of Human Genetics.



have been shaped by evolutionary forces. Therefore, well-powered eQTL mapping studies with large sample sizes in populations with African ancestry is critically needed to realize the potential and benefits of eQTL mapping studies across human populations.

To fill the above critical knowledge gap, here, we collected gene expression and genotype data from 1,032 African American (AA) samples and 801 European American (EA) samples from the Genetic Epidemiology Network of Arteriopathy (GENOA) study. We paired genotypes and gene expression data in these samples together to perform a comprehensive *cis*-eQTL mapping in both populations. By comparing eQTL mapping results in the two populations, our results reveal the genetic architecture differences underlying gene expression variation between African Americans and European Americans.

Material and Methods

Subjects

The Genetic Epidemiology Network of Arteriopathy (GENOA) is a community-based study of hypertensive sibships that was designed to investigate the genetics of hypertension and target organ damage. The study includes both African Americans (AA) from Jackson, Mississippi and European Americans (EA) from Rochester, Minnesota.¹⁸ In the initial phase of GENOA (phase I: 1996–2001), all members of sibships containing at least two individuals with essential hypertension clinically diagnosed before age 60 were invited to participate, including both hypertensive and normotensive siblings. Exclusion criteria for GENOA included secondary hypertension, alcoholism or drug abuse, pregnancy, insulin-dependent diabetes mellitus, or active malignancy. Eighty percent of AA ($n = 1,482$) and 75% of EA ($n = 1,213$) from the initial study population returned for the second examination (phase II: 2001–2005). Demographic information, medical history, clinical characteristics, lifestyle factors, and blood samples were collected in each phase. Written informed consent was obtained from all subjects and approval was granted by participating institutional review boards (University of Michigan, University of Mississippi Medical Center, and Mayo Clinic).

Genotyping Data and Quality Control

AA and EA blood samples were genotyped using either the Affymetrix Genome-wide Human SNP Array 6.0 platform or the Illumina Human1M-DUO Beadchip. For each platform, participants were excluded if they had an overall SNP call rate < 95% or sex mismatch between genotype and self-report. SNPs were excluded if they had a call rate < 95%. Principal component analysis was performed to identify and remove samples whose genotype profile appeared to be different from all other samples (outliers). After removing outliers, there were 1,599 AA samples and 1,464 EA samples with available genotype data. Imputation was performed using the Segmented HAPlotype Estimation & Imputation Tool (SHAPEIT¹⁹), v.2.r and IMPUTE v.2²⁰ using the 1000 Genomes project phase I integrated variant set release (v.3) in NCBI build 37 (hg19) coordinates (released on March 2012). Since genotyping was performed on multiple platforms, imputation was performed separately by platform and then the imputed data were combined. After imputation, SNPs with minor allele frequency (MAF) ≤ 0.01 or imputation

quality score (info score) ≤ 0.4 in any platform-based imputation were removed. The final set of genotype data included 30,022,375 and 26,079,446 markers for AA and EA, respectively, covering both SNPs and SNVs/indels. In our eQTL mapping analysis (more details below), we focused on genotype information for 6,432,684 imputed *cis*-SNPs on 1,032 AA individuals, and genotype information for 3,818,520 imputed *cis*-SNPs on 801 European American individuals that also have gene expression data.

In EA and AA separately, the GENESIS package in R was used to infer population structure.²¹ We used the PC-AiR function to extract the first five genotype PCs and used GEMMA²² to estimate an individual relatedness matrix. Both PCs and the relatedness matrix were included as covariates in the eQTL mapping analysis.

Gene Expression Data and Quality Control

Since eQTL architectures can change dynamically during the development and differentiation of cells, it is essential to map eQTLs in purified cell types.^{23,24} In our study, gene expression levels were measured using lymphoblastoid cell lines (LCLs) from a subset of AAs ($n = 1,233$) and EAs ($n = 919$) in order to minimize environmental influences. The gene expression levels of AA samples were measured using the Affymetrix Human Transcriptome Array 2.0 and those of EA samples were measured using the Affymetrix Human Exon 1.0 ST Array. We used the Affymetrix Expression Console provided by Affymetrix for array quality control and all array images passed visual inspection. In AA, we removed 28 samples due to either low signal-to-noise ratio ($n = 1$), abnormal polyadenylated RNA spike-in controls (Lys < Phe < Thr < Dap; $n = 24$), sample mislabeling ($n = 2$), or low RNA integrity ($n = 1$), leaving a total of $n = 1,205$ for analysis. In EA, we removed duplicated samples ($n = 31$), control samples ($n = 11$), and sex mismatch samples ($n = 2$), leaving $n = 875$ for analysis. We processed data in each population separately. Specifically, raw intensity data were processed using the Affymetrix Power Tool software.²⁵ Affymetrix CEL files were normalized using the Robust Multichip Average (RMA) algorithm which included background correction, quantile normalization, \log_2 -transformation, and probe set summarization.²⁶ The algorithm also includes GC correction (GCCN), signal space transformation (SST), and gain lock (value = 0.75) to maintain linearity. The Brainarray custom CDF²⁷ version 19 (see [Web Resources](#)) was used to map the probes to genes. This custom CDF²⁷ uses updated genomic annotations and multiple filtering steps to ensure that the probes used are specific for the intended gene cluster. In particular, it removes probes with non-unique matching cDNA/EST sequences that can be assigned to more than one gene cluster. Consequently, the gene expression data processed through the custom CDF in²⁷ is expected to be largely free of mappability issues. However, we do acknowledge that alignment bias may still exist due to genetic variation, errors in the reference genome and other complications.²⁸ After mapping, we used ComBat software²⁹ to remove batch effects. Finally, the gene expression data were quantile normalized across genes for the following eQTL analysis. A total of 17,616 autosomal protein-coding genes in AA and 17,360 autosomal protein-coding genes in EA were available for analysis. In AA samples 17,572 genes and in EA samples 17,343 genes were mapped to the corresponding imputed SNPs.

eQTL Mapping Analysis

The eQTL mapping analysis was performed in AA and EA samples separately, using individuals with both genotype and

gene expression data ($n = 1,032$ in AA and $n = 801$ in EA). For each gene, we first extracted *cis*-SNPs that are within 100 kb of transcription start site or transcription end site of genes, following recommendations by Peters et al.³⁰ A total of 17,572 genes in AA and a total of 17,343 genes in EA had non-zero *cis*-SNPs. The median number of *cis*-SNPs per gene is 722 for AA (mean = 825.8; SD = 649.8) and 418 for EA (mean = 491.4, SD = 410.8), with range varying from 1 to 19,808 for AA and from 1 to 13,379 for EA. We focused our analysis on genes with at least one *cis*-SNP. For each gene, we then applied a linear mixed model implemented in GEMMA²² for eQTL mapping, adjusting for age, gender, the top five genotype PCs from PC-AiR, and the genetic relatedness matrix from GEMMA. Afterward, we selected the SNP with the lowest p value for each gene as the candidate eQTL and used its p value as the gene-level significance measure. We permuted the sample labels ten times and applied the same eQTL mapping procedure to obtain an empirical null distribution of gene-level p values.^{31–33} In each population, after each permutation, we kept the most significant p value per gene. With the empirical null distribution, we computed the false discovery rate (FDR) associated with each p value threshold following Barreiro et al.³¹ and Pickrell et al.³² and selected the p value threshold that provided a 5% FDR control. The p value threshold used is $6.245907e-05$ in AA and $1.385504e-4$ in EA. We refer to the genes that pass an FDR threshold of 5% as the identified eGenes and refer to the SNPs with the lowest p value in these genes as the identified (primary) eQTLs. We refer to the significant *cis*-SNPs in the eGenes as eSNPs. We also used Plink³⁴ to calculate Weir and Cockerham's F_{st} ³⁵ to measure the degree of population differentiation between AA and EA. Negative values of Weir and Cockerham's F_{st} were treated as zero. The summary statistics from eQTL mapping analysis along with all analysis scripts are available on our website (see [Web Resources](#)).

We examined the overlap of the detected eGenes and eSNPs in AA or EA in other replication cohorts (AFA, CAU, and HIS in MESA; YRI and EUR in Geuvadis; details of these populations are described below). In particular, we used the qvalue method^{36,37} to estimate the expected true positive rate π_1 between populations. The π_1 statistics was estimated by selecting the SNP-gene pairs with $FDR \leq 0.05$ in AA or EA population from the GENOA cohort and examining their p value distribution in each replication cohort (YRI and EUR in Geuvadis, AFA, CAU, HIS in MESA). π_0 is the proportion of false positives estimated by assuming a uniform distribution of null p values and $\pi_1 = 1 - \pi_0$.³⁷

For each eGene in turn, we performed conditional analysis to identify additional conditional eQTLs following Jansen et al.³³ To do so, we refer to the primary eQTLs as E1 SNPs. For each gene in turn, we performed association analysis conditional on the E1 SNP and identified the strongest SNP association among the remaining SNPs. We refer to the identified SNP as an E2 SNP if its conditional p value is below the genome-wide significance threshold established in the above paragraph. Afterward, we performed further association analysis conditional on both E1 and E2 SNPs to identify E3 SNPs. We repeated such process until the smallest p value among the remaining SNPs can no longer exceed the genome-wide significance threshold.

We performed subsampling analysis to check whether gene length is a potential source of bias in eQTL detection. In the first analysis, we focused on half of the genes that have a SNP number greater than or equal to the median value (8,802 genes in AA and 8,694 genes in EA). For each gene in turn, we down-sampled its *cis*-SNPs to the median value, so that all genes have the same num-

ber of *cis*-SNPs. In the second analysis, we focused on the genes with SNP density higher or equal to the median (8,787 genes in AA and 8,672 genes in EA). The SNP density is defined as the ratio between the number of SNPs in a gene and the length of that gene. Afterward, for each gene in turn, we randomly subsampled a specific number of SNPs to do the analysis, while the specific number is selected as the median SNP density multiple the gene length. For both subsampling analyses, we repeated the down-sampling procedure 10 times and averaged results to account for stochasticity in the down-sampling process.

Controlling for Local Ancestry

We performed local ancestry (LA) inference in AA and EA samples using the software Efficient Local Ancestry Inference (ELAI) v.1.01³⁸ in the FRANC interface (see [Web Resources](#)). We used the default settings in ELAI. We downloaded genotype files in plink format for 83 Utah Residents (CEPH) with Northern and Western European Ancestry (CEU) and 88 Yoruba in Ibadan, Nigeria (YRI) populations from the 1000 Genomes Project to serve as reference panels. We focused on the common set of autosomal SNPs that are available both in the 1000 Genomes Project and in the AA or EA samples for ancestry inference. We converted variant base pair positions to centimorgans using the hg19 genetic map. The inferred local ancestry is in the value of the number of African ancestry alleles (0, 1, or 2) for each SNP. We treated these inferred values as an additional covariate in the eQTL mapping using the LAMatrix R package.³⁹ Note that the LAMatrix software is not able to control for family relatedness in GENOA. In the analysis, we also constructed empirical null distributions as described above, computed the false discovery rate (FDR) associated with each p value threshold, and selected the p value threshold that provided a 5% FDR control. Such p value threshold is $5.962974e-05$ in AA and $1.376416e-4$ in EA. As described above, we refer to genes that pass an FDR threshold of 5% as the identified eGenes and refer to the SNPs with the lowest p value in these genes as the identified (primary) eQTLs. We also refer to the significant *cis*-SNPs in the eGenes as eSNPs.

Gene Expression Heritability Estimation and Partitioning

For each gene, we estimated the proportion of variance in gene expression level explained by all SNPs using the Bayesian sparse linear mixed model (BSLMM) implemented in GEMMA. Following Mogil et al.,¹⁴ we also used BSLMM⁴⁰ to partition the gene expression variance into a *cis*-component that is explained by *cis*-SNPs and a *trans*-component that is explained by *trans*-SNPs. To do so, for each gene we fit the following model:

$$y = \mu + x_{cis}\beta_{cis} + x_{trans}\beta_{trans} + \epsilon$$

$$\beta_{cis,i} \sim \pi N(0, \sigma_a^2) + (1 - \pi)\delta_0$$

$$\beta_{trans,i} \sim N(0, \sigma_b^2)$$

Where y is a n by 1 vector of gene expression levels for n individuals; μ is the intercept; x_{cis} is the n by p_{cis} matrix of genotypes for p_{cis} *cis*-SNPs of interest and β_{cis} are the corresponding effect sizes; x_{trans} is the n by p_{trans} matrix of genotypes for p_{trans} *trans*-SNPs of interest (i.e., SNPs that are not *cis*-SNPs); and β_{trans} are the corresponding effect sizes, here p_{trans} was based on all genotyped sites used in our analyses; and ϵ is a n by 1 vector of residual errors.

We used 1,000 burn-in steps and 10,000 sampling steps in the Markov chain Monte Carlo (MCMC) algorithm to fit BSLMM. We used the posterior samples of β_{cis} and β_{trans} to calculate $V(x_{cis}\beta_{cis})/V(y)$, which represents the proportion of variance in the phenotype explained by *cis*-SNPs, as well as $V(x_{trans}\beta_{trans})/V(y)$, which represents the proportion of variance in the phenotype explained by *trans*-SNPs. Besides the main analysis where we used all *trans*-SNPs, we also performed sensitivity analysis where we used only *trans*-SNPs that reside on different chromosomes.

Conservation Scores

We obtained three types of conservation scores: phyloP score,⁴¹ phastCons score,⁴² and dN/dS ratio.⁴³ The phyloP score measures the evolutionary conservation at each individual alignment site and the absolute phyloP score is a $-\log p$ value for testing the null hypothesis of neutral evolution. A positive sign of phyloP score indicates conservation and slower evolution than expectation, while a negative sign of phyloP score indicates faster evolution than expectation.⁴⁴ The phastCons score measures the probability that each nucleotide belongs to a conserved element and aims to compare whether the site is better explained by the conserved model or by the non-conserved model. A higher phastCons score represents more conservation.⁴² The dN/dS score measures the direction and magnitude of nature selection on the protein-coding genes. A dN/dS ratio greater than 1 implies positive selection; a ratio less than 1 implies negative selection; while a ratio of exactly 1 indicates no selection.⁴⁵ We obtained the per-site phyloP and phastCons scores from the 100-way vertebrate comparison on the UCSC Genome Browser⁴⁶ for each base position inside the annotated exons and averaged them to obtain the per-gene phyloP and phastCons scores. We obtained per-gene dN and dS scores using the BioMart R package.⁴⁷

We compared the conservation scores in eGenes that are identified in both populations, eGenes that are uniquely identified in one population, and non-eGenes. We performed Jonckheere-Terpstra test to test whether there is an observable trend in conservation scores across these three classes of genes.

Functional Enrichment Analysis

We performed GO and KEGG pathway enrichment analyses to investigate the shared biological function among eGenes in the AA and EA populations. We do so by using the g:GOST tool on the web software g:Profiler and used the expressed genes as background.⁴⁸ In the analysis, we used the default option g:SCS method in g:Profiler for multiple testing correction. We presented pathways identified with an adjusted p value $< 1e-5$. To adjust for the potential influence of gene length to the GO analysis, we also carried out GO enrichment using R package GOfuncR.^{49,50} In the analysis, we computed family-wise error rates (FWER) based on permutations of gene-associated variables and used an FWER threshold of 0.1 to declare enrichment significance.

Comparison of eQTL Results with Previous Studies

We compared our findings (eGenes, eSNPs, and eQTLs) to those from two previous eQTL mapping studies. These two previous studies include the Geuvadis Consortium study⁸ and the Multi-Ethnic Study of Atherosclerosis (MESA).¹⁴ The Geuvadis study was performed on lymphoblastoid cell lines (LCL) of 465 individuals from five different populations: Utah residents (CEPH) with northern and western European ancestry (CEU, $n = 92$), Finns

(FIN, $n = 95$), British (GBR, $n = 96$), Toscani (TSI, $n = 93$), and Yoruba (YRI, $n = 89$). The MESA study was performed on CD14⁺ monocytes of individuals from three different populations: African American (AFA, $n = 233$), Hispanic (HIS, $n = 352$), and European (CAU, $n = 578$). In the Geuvadis results, we directly matched their reported Ensembl gene IDs to GENOA and matched SNPs between studies through their positions. In the MESA data, we directly matched their reported Ensembl gene IDs to GENOA and matched SNPs between studies through matching rs IDs.

Gene Expression Prediction

We constructed gene expression prediction models using AA and EA samples in either GENOA or MESA. We then accessed the prediction performance of these models in a separate study, the Geuvadis study. For MESA, we directly downloaded the *cis*-SNP weights. These weights were produced by fitting the elastic net model for gene expression prediction with PrediXcan in the MESA study.¹⁴ For GENOA, we followed the MESA study¹⁴ and used the glmnet R package⁵¹ to fit the elastic net model for gene expression prediction. Also following the MESA study, we set elastic net regularization penalty $\alpha = 0.5$. Besides using the elastic net, we also used BSLMM⁴⁰ for gene expression prediction. After building expression prediction models in either MESA and GENOA, we downloaded individual-level genotype and gene expression data from Geuvadis and examined the prediction performance there. To do so, we processed the Geuvadis gene expression data as described in Lappalainen et al.⁸ Specifically, we focused our analysis on protein-coding genes that are annotated from GENCODE⁵² (release 12). We removed lowly expressed genes that have zero counts in at least half of the individuals and retained a total of 15,810 genes. Afterward, we performed PEER normalization to remove confounding effects and unwanted variations.⁵³ In order to remove potential population stratification in Geuvadis, we quantile normalized the gene expression measurements across individuals in each population to a standard normal distribution, and then quantile normalized the gene expression measurements to a standard normal distribution across individuals from all five populations. In addition to the gene expression data, all individuals in Geuvadis also have their genotypes sequenced in the 1000 Genomes project. Among the sequenced genotypes, we retained 7,072,917 SNPs that have a MAF above 0.05. We compared the prediction performance in a set of 2,524 common genes across all seven prediction models (GENOA AA and EA with BSLMM and elastic net; MESA AFA, CAU, and HIS with elastic net). We predicted the expression level of each gene in the Geuvadis data using the *cis*-SNP weights constructed in either GENOA or MESA, with overlap SNPs between GENOA and Geuvadis and between MESA and Geuvadis. We then measured the prediction performance using the squared Pearson's correlation coefficient (R^2) between the predicted expression level and true expression level as described in Mikhaylova and Thornton.⁵⁴

TWAS Analysis in WTCCC

The Wellcome Trust Case Control Consortium (WTCCC) study⁵⁵ data consist of about 14,000 case subjects from seven common diseases and 2,938 shared control subjects. The cases include 1,963 individuals with type 1 diabetes (T1D [MIM: 222100]), 1,748 individuals with Crohn disease (CD [MIM: 266600]), 1,860 individuals with rheumatoid arthritis (RA [MIM: 180300]), 1,868 individuals with bipolar disorder

Table 1. Comparison of eQTL Mapping Results for African Americans and European Americans in the GENOA Study

	African American (AA)			European American (EA)			Overlapping		
	Number	Total	Percentage	Number	Total	Percentage	Number	AA%	EA%
eGenes	5,475	17,572	31.16%	4,402	17,343	25.38%	3,048	55.67%	69.24%
eSNPs	354,931	14,511,338	2.45%	371,309	8,521,801	4.36%	112,316	31.64%	30.25%

The first row shows the number of eGenes that are identified in AA (first column), the total number of genes analyzed in AA (second column), the percentage of genes that are eGenes in AA (third column), the number of eGenes that are identified in EA (fourth column), the total number of genes analyzed in EA (fifth column), the percentage of genes that are eGenes in EA (sixth column), the number of common eGenes identified in both AA and EA (seventh column), the proportion of eGenes identified in AA that are also identified in EA (eighth column) and the proportion of eGenes identified in EA that are also identified in AA (ninth column), at FDR ≤ 0.05 .

(BD [MIM: 125480]), 1,924 individuals with type 2 diabetes (T2D [MIM: 125853]), 1,926 individuals with coronary artery disease (CAD [MIM: 608320]), and 1,952 individuals with hypertension (HT [MIM: 145500]). We obtained quality-controlled genotypes from WTCCC and imputed missing genotypes using BIM-BAM.⁵⁶ We obtained a total of 458,868 SNPs shared across all individuals. We then imputed SNPs based on the 1000 Genomes project reference panel using SHAPEIT and IMPUTE2.²⁰ For TWAS analysis, we focused on genes and SNPs that are shared between WTCCC and GENOA or shared between WTCCC and MESA. We calculated the predicted gene expression levels in WTCCC using models constructed either in GENOA (BSLMM or elastic net) or MESA (elastic net), with details described in the previous section. We then tested for association between the predicted gene expression level and disease status using logistic regression, with the first ten genetic PCs included as covariates. We considered the association between gene and disease genome-wide significant if its p value is below the Bonferroni corrected genome-wide threshold of 0.05. For results validation, for each prediction model in turn, we counted the number of genes identified in each WTCCC trait (T1D, T2D, RA, HT, CD, CAD, and BD) that is replicated in post-WTCCC studies. In particular, we defined replication as the genes within 100 kb of a previous gene reported to be associated with the same trait in the GeneCards knowledge base.⁵⁷

Results

eQTL Mapping in AA and EA Samples in the GENOA Study

We performed eQTL mapping in the GENOA study in the AA and EA samples separately. The description of the GENOA study, the gene expression data collection and processing procedure, the genotype data collection and processing procedure, and the eQTL mapping procedure are all provided in [Material and Methods](#). Briefly, the AA data include expression measurements for 17,616 protein-coding genes and genotype information for 30,022,375 imputed SNPs for 1,032 AA individuals. The EA data include 17,360 protein-coding genes and genotype information for 26,079,446 imputed SNPs for 801 EA individuals. We processed gene expression data with Combat²⁹ to remove batch effects or other technical covariates. We extracted *cis*-SNPs within 100 kb of each gene and used linear mixed models implemented in GEMMA for eQTL mapping.²² In the analysis, we adjusted for age, gender,

the top five genetic principal components (PCs), as well as a genetic relatedness matrix to control for familial relationships. Note that, following previous approaches,⁵⁸ we determined the number of genotype PCs included in the model based on maximizing the number of discoveries ([Figure S1](#)). Overall, we examined a total of 17,572 genes and 6,432,684 unique *cis*-SNPs, with an average of 825.8 *cis*-SNPs per gene in the AA samples; and 17,343 genes and 3,818,520 unique *cis*-SNPs, with an average of 491.4 *cis*-SNPs per gene in the EA samples. Following Tung et al.,⁵⁹ we refer to a gene that harbors at least one eQTL as an eGene. We used an empirical gene-level FDR threshold of 5% constructed across all genes for identifying eGenes. Following Tung et al.,⁵⁹ we refer to the lowest p value SNP in each eGene as the (primary) eQTL. Following Barreiro et al.³¹ and Pickrell et al.,³² we refer to any *cis*-SNP with a significant association with the eGene as an eSNP. We used the p value threshold corresponding to the same empirical FDR of 5% for eGene detection to declare eSNPs. Besides this primary analysis, we also performed conditional analysis to identify additional eQTLs (more in the following section). The summary statistics from eQTL mapping analysis and all analysis scripts are available on our website (see [Web Resources](#)).

In total, we identified 5,475 eGenes in the AA samples and 4,402 eGenes in the EA samples, with 3,048 overlapping between AA and EA (overlapping Jaccard index = 0.446; [Table 1](#) and [Figure 1D](#)). We also identified a total of 354,931 eSNPs in AA and 371,309 eSNPs in EA, with 112,316 eSNPs overlapping between the two populations (overlapping Jaccard index = 0.183). The proportion of overlapped eGenes increases from 53.01% to 59.15% in AA and increases from 66.81% to 69.05% in EA when the FDR threshold is increased from 0.01 to 0.2, though the proportion of overlapped eSNPs remains similar ([Table S1](#)). The lack of complete overlap of eGenes or eSNPs between the two populations is in part due to statistical power and in part due to the difference in the genetic architecture underlying gene expression levels between populations. In addition, our results are largely consistent with previous studies, with many eSNPs and eGenes in previous studies replicated in our study. Specifically, compared to the Geuvadis study,⁸ 81.01% of eGenes and 84.01% of eSNPs identified in the Yoruba (YRI) population (n = 89) are also identified in our AA samples. In addition,

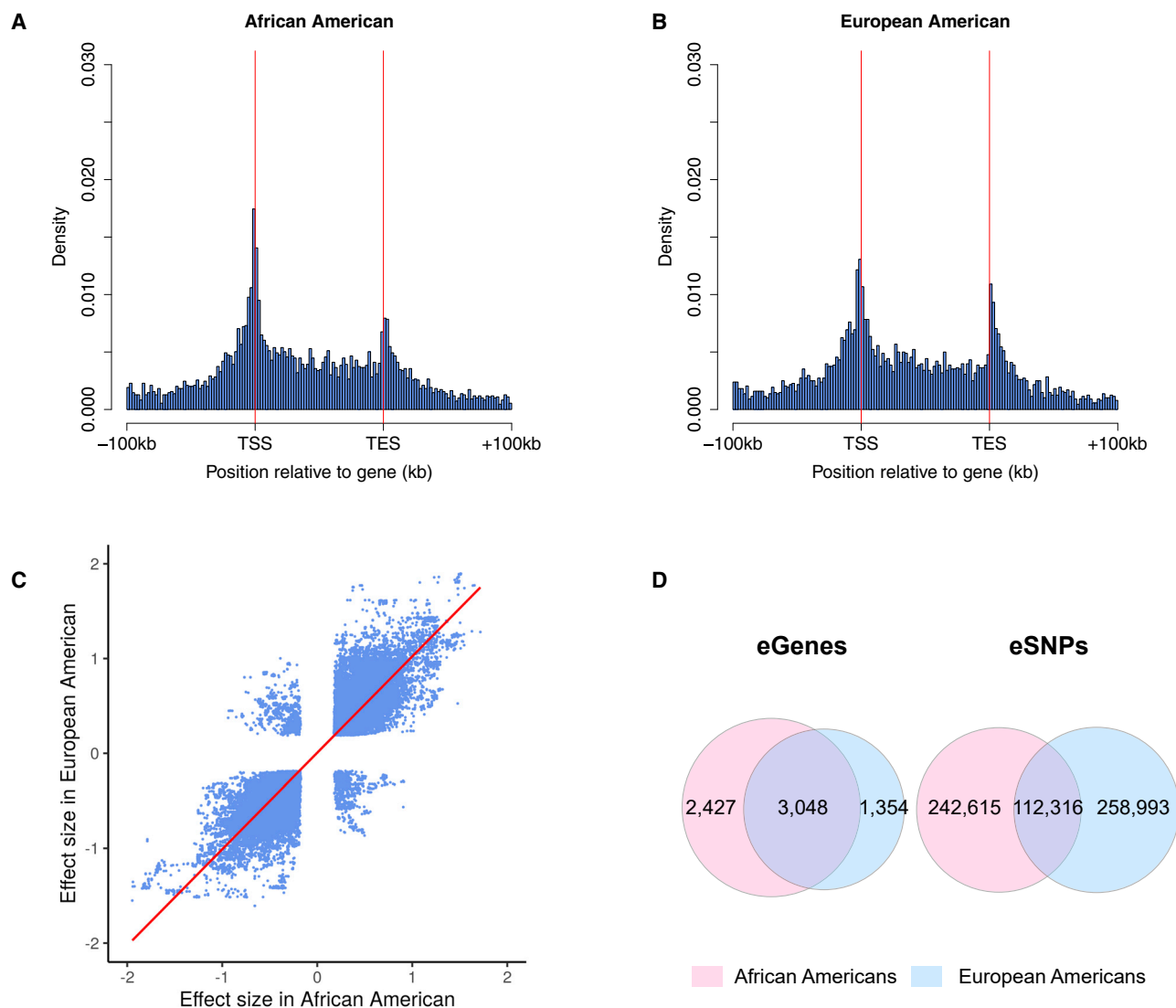


Figure 1. Overview of eQTL Mapping Results in GENOA

(A) The locations of the eQTLs in the eQTL analysis are shown relative to the most 5' gene transcription start site (TSS) and the most 3' gene transcription end site (TES) for each of the 5,475 eGenes in AA.

(B) The locations of the eSNPs are shown relative to the most 5' TSS and the most 3' TES for each of the 4,402 eGenes in EA.

In both (A) and (B), identified eQTLs are enriched near TSS, TES, and gene body. For SNPs residing between TSS and TES, we scaled its distance to the transcript starting site by gene length.

(C) The effect size and direction of effect for the shared gene-SNP pairs (112,316) between AA and EA are highly consistent.

(D) Venn diagram plots show the overlap of eGenes and eSNPs identified in AA and EA.

65.39% of eGenes and 63.4% of eSNPs identified in the European (EUR) population in Geuvadis ($n = 373$) are also identified in our EA samples (Table 2). Compared to the MESA study (AFA: $n = 233$; CAU: $n = 578$; HIS: $n = 352$),¹⁴ 32.21% of eGenes and 24.89% of eSNPs identified in their AFA population are also identified in our AA samples. Also, 31.23% of eGenes and 19.33% of eSNPs identified in the CAU population in the MESA study are also identified in our EA samples (Table 3). However, our analysis also identified many new eGenes and eSNPs that were not identified in these previous studies. For example, compared to the Geuvadis study,⁸ we identified 4,271 new eGenes and 22,506 new eSNPs in our AA samples than that in the YRI population; 2,116 new eGenes and 55,017 new

eSNPs in our EA samples than that in the EUR population. Similarly, compared to the MESA study, we identified 2,345 new eGenes and 146,651 new eSNPs in our AA samples as compared to that in the AFA samples; and 1,220 new eGenes and 99,298 new eSNPs in our EA samples as compared to that in the CAU samples. We also examined the true positive rate π_1 of the detected eSNPs in the AA or EA populations that are replicated in the MESA and Geuvadis studies. The results show the true positive rate of eSNPs is in the range of 59.3%–91.9% in AA (with values varying based on which population the comparison is performed on) and that in the 51.4%–90.9% in EA (Table S2). Certainly, a lack of complete overlap of eGenes or eSNPs among different studies is expected, given that statistical

Table 2. Comparison of eQTL Mapping Results between GENOA and Geuvadis

	Genes (or Gene-SNP Pairs) Analyzed in Both Studies	Detected in Geuvadis	Detected in GENOA	Overlapped between the Two Studies
GENOA AA (n = 1,205) versus Geuvadis YRI (n = 89)				
eGenes	10,539	416	4,608	337
eSNPs	51,611	7,791	29,051	6,545
GENOA EA (n = 801) versus Geuvadis EUR (n = 373)				
eGenes	11,130	2,800	3,947	1,831
eSNPs	331,784	159,262	156,027	101,010

The first row shows the number of eGenes that are identified in GENOA AA and analyzed in Geuvadis YRI (first column), the number of eGenes in AA that are also eGenes in Geuvadis YRI (second column), the percentage of also eGenes in Geuvadis YRI that are also eGenes in AA (third column), the number of eGenes that are identified in GENOA EA and analyzed in Geuvadis EUR (first column), the number of eGenes in EA that are also eGenes in Geuvadis EUR (second column), the percentage of also eGenes in Geuvadis EUR that are also eGenes in EA (third column).

power is unlikely achieved fully in any study and that different studies differ in terms of the *cis* window size, used tissue types (e.g., MESA uses monocytes while the others use LCLs) as well as applied FDR methods (e.g., permutation based versus Benjamini-Hochberg).

We used ELAI to infer local ancestry and treated the inferred local ancestry as covariates in the eQTL mapping analysis using the LAMatrix package. We found that the eQTL mapping results controlling for local ancestry are largely consistent with the main results. Specifically, after adjusting for local ancestry, we identified 5,553 eGenes in AA and 4,586 eGenes in EA, with 5,312 and 4,333 genes overlapped with the main results (overlapping Jaccard index = 0.929 in AA and 0.931 in EA; Table S3). We identified a total of 357,072 eSNPs in AA and 372,240 eSNPs in EA, with 325,571 and 347,949 eSNPs overlapped with the main results (Jaccard index = 0.843 in AA and 0.880 in EA). The estimated effect sizes after adjusting for local ancestry are highly correlated with the main results (Pearson's correlation = 0.991, p value < $2.23e-308$ in AA; correlation = 0.994, p value < $2.23e-308$ in EA; Figure S2). In addition, the $-\log_{10}$ p values are also highly correlated between these two approaches (Spearman's correlation = 0.963, p value < $2.23e-308$ in AA; correlation = 0.972, p value < $2.23e-308$ in EA; Figure S3).

Characteristics of eGenes and eQTLs

We first examined the properties of the identified eQTLs and eSNPs. As expected,⁶⁰ the eQTLs identified in both AA and EA samples are strongly enriched near gene transcription start sites, inside gene bodies, and near transcription end sites (Figures 1A and 1B), validating the eQTL mapping results. Within each population, the absolute eQTL effect size is negatively correlated with its minor allele frequency (MAF) (Pearson coefficient = -0.47 , p value < $2.23e-308$ in AA; Pearson coefficient = -0.46 , p value < $2.23e-308$ in EA; Figures S4A and S4B), likely reflecting either winner's curse or negative selection.⁵⁹ In addition, the significance level of the eQTLs in terms of $-\log_{10}$ p value is positively correlated with MAF in each of the two populations (Spearman's coefficient = 0.414, p value < $2.23e-308$ in AA; Spearman's coef-

ficient = 0.341, p value < $2.23e-308$ in EA), likely reflecting the increased power with increasing MAF. Between populations, the $-\log_{10}$ (p value) difference between the two populations is positively correlated with MAF difference (Spearman's correlation = 0.07, p value < $2.23e-308$; Figure S5). The average MAF difference between AA and EA is -0.0133 in non-eSNPs (Wilcoxon test p value < $2.23e-308$), 0.0396 in AA-specific eSNPs (p value < $2.23e-308$), -0.0496 in EA-specific eSNPs (p value < $2.23e-308$), and -0.0053 in common eSNPs (p value = $9.15e-27$; Figures S6 and S7), suggesting that AA-specific eSNPs tend to have higher MAF in AA than in EA while the EA-specific eSNPs tend to have higher MAF in EA than in AA. Consistent with Glassberg et al.,⁶¹ we also found that eSNPs tend to have higher MAF as compared to tested SNPs in both AA and EA (Figure S8). Besides the influence of MAF on power, we found that the effect sizes of the identified common eSNPs shared between EAs and AAs are highly correlated with each other (Pearson coefficient = 0.903; p value < $2.23e-308$; Figure 1C), with 97.3% of eSNPs sharing the same effect sign between AA and EA. The significance level in terms of $-\log_{10}$ p value of the corresponding eSNPs in the two populations are also positively correlated (Spearman's coefficient = 0.42, p value < $2.23e-308$), partially reflecting the MAF correlation between the two populations (Pearson coefficient = 0.35, p value < $2.23e-308$). In addition, we found that EA unique eSNPs tends to have larger effect size in EA as compared to AA, and vice versa (Figure S9). The primary eQTLs also tend to have the largest effect size across all *cis*-SNPs for a given gene: in AA, 428 (7.8%) out of the 5,475 primary eQTLs have the largest effect sizes (versus 0.15% by chance alone); in EA, 488 (11.09%) out of 4,402 primary eQTLs also have the largest effect sizes (versus 0.27% by chance alone). In addition, in AA, 1,105 (20.18%) out of the 5,475 primary eQTLs have the largest MAF across all SNPs mapped to a given gene. In EA, 715 (16.24%) out of 4,402 primary eQTLs also have the largest MAF across all SNPs mapped to a given gene.

We next examined the properties of the identified eGenes. Within each population, we first found that eGenes with longer length tended to have a higher number

Table 3. Comparison of eQTL Mapping Results between GENOA and MESA

	Genes (or Gene-SNP Pairs) Analyzed in Both Studies	Detected in MESA	Detected in GENOA	Overlapped between the Two Studies
GENOA AA (n = 1,205) versus MESA AFA (n = 233)				
eGenes	9,221	4,275	3,722	1,377
eSNPs	5,038,835	197,277	195,747	49,096
GENOA EA (n = 801) versus MESA CAU (n = 578)				
eGenes	9,151	5,559	2,956	1,736
eSNPs	3,154,038	533,989	202,503	103,205

The first row shows the number of eGenes that are identified in GENOA AA and analyzed in MESA AFA (first column), the number of eGenes in AA that are also eGenes in MESA AFA (second column), the percentage of also eGenes in MESA AFA that are also eGenes in AA (third column), the number of eGenes that are identified in GENOA EA and analyzed in MESA CAU (first column), the number of eGenes in EA that are also eGenes in MESA CAU (second column), the percentage of also eGenes in MESA CAU that are also eGenes in EA (third column).

of eSNPs (p value in AA = $7.9e-04$; p value in EA = $1.7e-3$) but a lower density of eSNPs (p value in AA = $2.51e-13$; p value in EA = $1.81e-8$). Because we defined eGenes as genes that harbor at least one significant eSNP, longer genes with a larger number of SNPs will tend to be eGenes. Therefore, we performed subsampling-based analyses to avoid such potential confounding and more carefully examine the property of eGenes in terms of their gene length and SNP density (details in [Material and Methods](#)). The first subsampling analysis ensures that all analyzed genes have the same number of *cis*-SNPs. In such analysis, we found that the lowest p value for each gene is negatively correlated with gene length (before subsampling: Spearman's correlation = -0.146 and -0.141 in AA and EA; p value = $2.31e-43$ and $4.77e-40$; after subsampling: correlation = -0.107 and -0.109 ; p value = $6.04e-24$ and $1.9e-24$) while positively correlated with SNP density (before subsampling: correlation = 0.135 and 0.118 ; p value = $3.48e-37$ and $3.66e-28$; after subsampling: correlation = 0.103 and 0.094 ; p value = $2.45e-22$ and $1.912e-18$), consistent with our above conclusion (note that a negative correlation between p value and gene length means that an eGene tends to have longer gene length). The second subsampling analysis ensures that all analyzed genes have the same SNP density. In such analysis, we found that the lowest p value for each gene is also negatively correlated with gene length (before subsampling: Spearman's correlation = -0.267 and -0.269 in AA and EA; p value = $3.99e-143$ and $7.13e-144$; after subsampling: correlation = -0.458 and -0.425 ; p value < $2.23e-308$ and < $2.23e-308$). Overall, these subsampling-based analyses support the conclusion that an eGene tends to have a longer gene length and lower SNP density.

Next, between populations, we found that the common eGenes shared between the two populations are often less evolutionarily conserved than unique eGenes that are identified in a single population, which are also less evolutionarily conserved than non-eGenes. This decreased conservation pattern in non-eGenes versus unique eGenes versus common eGenes can be clearly visualized using each of the three commonly used conservation scores: phyloP (p value = $1.86e-07$; [Figure 2A](#)), phastCons

(p value = $1.6e-35$; [Figure 2B](#)), and dN/dS ratio (p value = $2.94e-10$; [Figure 2C](#)). For example, the mean phyloP score is 0.255, 0.207, 0.228, and 0.166, for non-eGenes, eGenes unique to EA, eGenes unique to AA, and eGenes shared between the two populations, respectively. The corresponding mean phastCons scores are 0.151, 0.135, 0.133, and 0.117 and the corresponding mean dN/dS ratios are 0.135, 0.127, 0.131, and 0.144. The decreased conservation in common eGenes shared between populations dovetails an early study in primates.⁵⁹ In addition, we found that eSNPs in AA and EA tended to have a higher F_{st} value than non-eSNPs, supporting the previous observation that eSNPs are more variable than non-eSNPs¹³ ([Figures 2D](#), [S10A](#), and [S10B](#)). The mean F_{st} for the eSNPs shared between EA and AA, eSNPs unique to either EA or AA, and non-eSNPs are 0.0888, 0.079, 0.0895, and 0.0338, respectively ([Figure 2D](#)).

We also performed a gene ontology (GO) analysis on eGenes versus non-eGenes to examine whether eGenes are enriched in particular pathways (details in [Material and Methods](#)). We found that, in both EA and AA, the eGenes are highly enriched in catalytic activity, protein binding, and transferase activity among the GO molecular functions ([Tables S4](#) and [S8](#)); are enriched in metabolic processes among the GO biological processes ([Tables S5](#) and [S9](#)); and are enriched in intracellular part, cytoplasmic part, and mitochondrion among the GO cellular components ([Tables S6](#) and [S10](#)). In human phenotype ontology analysis, we found that eGenes are enriched in autosomal-recessive inheritance in both AA and EA ([Tables S7](#) and [S11](#)). The GO analysis results are consistent with the previous finding that eGenes tend to be less conserved, are enriched for targets of purifying selection, and are more likely to be observed in recessive disorders.^{62,63} In addition, the GO enrichment using R package GOfuncR^{49,50} that controls for the influence of gene length also yields consistent results ([Tables S20–S22](#)).

Gene Expression Heritability Estimation and Partitioning

Next, we estimated the genetic architecture underlying gene expression variation through heritability estimation and partitioning. For each gene in turn, we estimated the

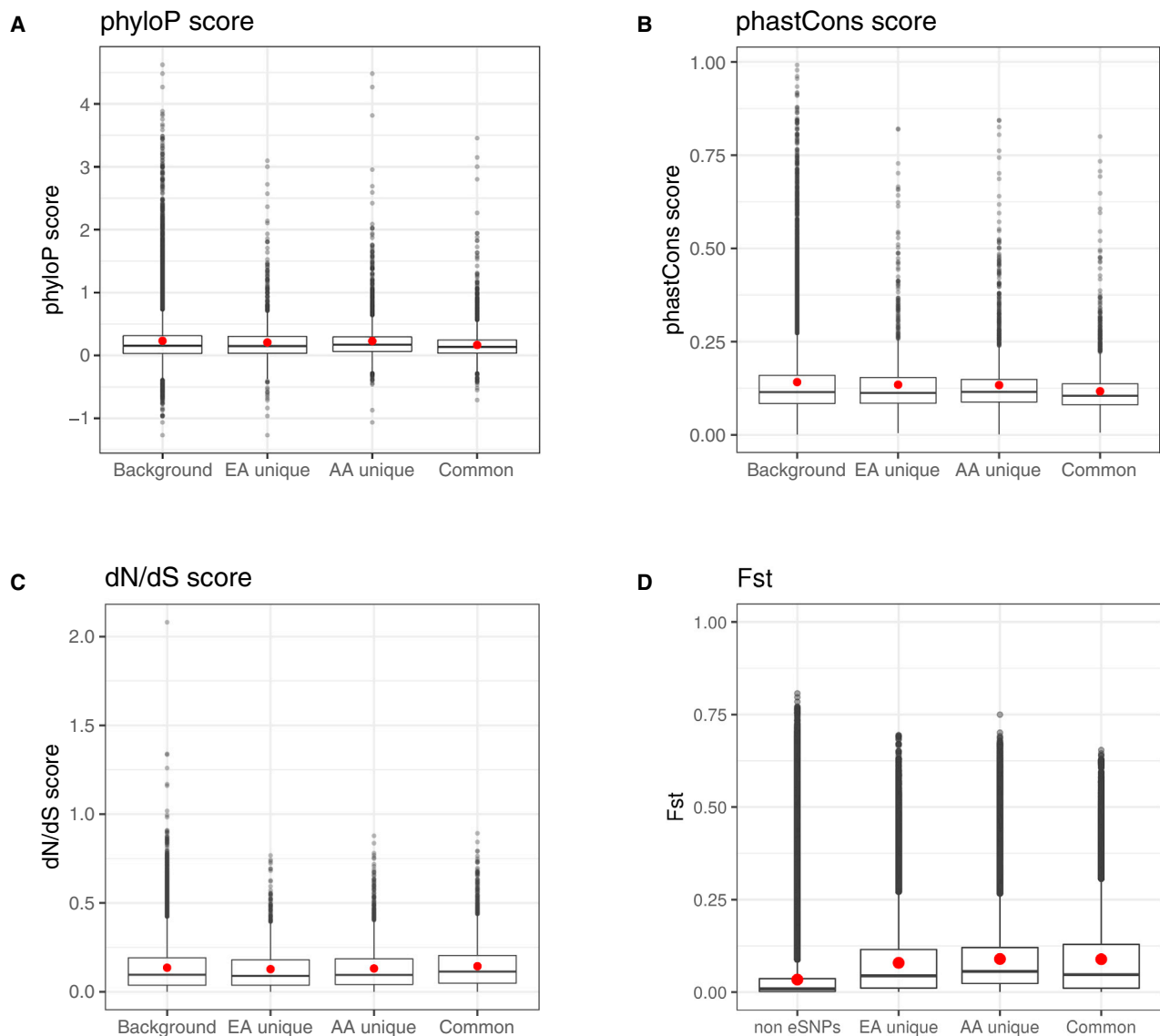


Figure 2. The Relationship between Conservation Scores and Four Categories of Genes

(A) Boxplot of phyloP scores, together with the mean (red dot), across four groups of genes: eGenes that are shared between EA and AA; eGenes that are unique to either EA or AA; non-eGenes. phyloP scores are based on a 100-way primate genome comparison.

(B) Boxplot of phastCons scores, together with the mean (red dot), across the same four groups of genes. phastCons scores are based on a 100-way primate genome comparison.

(C) Boxplot of dN/dS ratio, together with the mean (red dot), across the same four groups of genes.

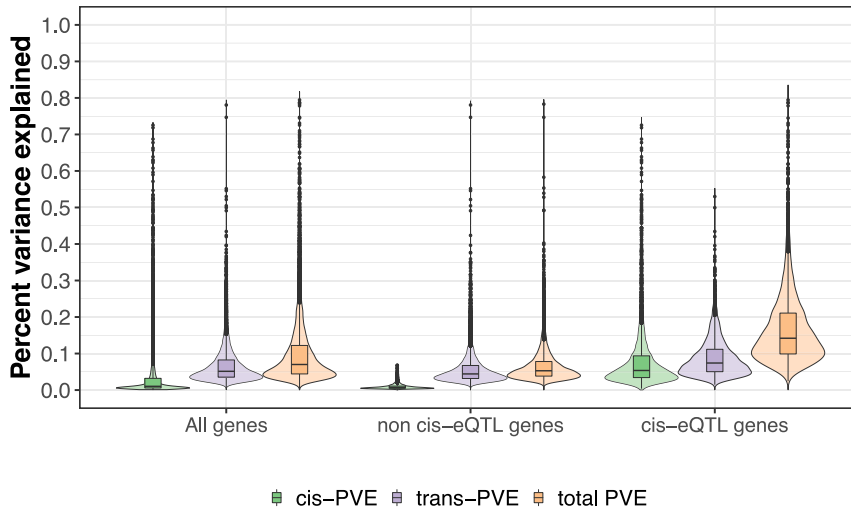
(D) Boxplot of F_{st} , together with the mean (red dot), across the same four groups of genes.

Note that a high phyloP score, a high phastCons score, or a low dN/dS ratio represents the gene is more conserved. The results show that the non-eGenes, which are treated as background genes, are most conserved. The eGenes unique in either European Americans (EA unique) or African Americans (AA unique) are less conserved. The common eGenes between European Americans and African Americans are the least conserved. The Jonckheere-Terpstra tests for testing such trend are significant for all these scores: p value = $2.94e-10$ for dN/dS score; p value = $1.86e-07$ for phyloP; p value = $1.6e-35$ for phastCons; and p value < $2.23e-308$ for F_{st} . Again, the red dots represent the mean values in each boxplot.

proportion of variance (PVE) in gene expression levels that are accounted for by all SNPs using the Bayesian sparse linear mixed model (BSLMM). This quantity is commonly referred to as SNP heritability. We used Benjamini-Hochberg false discovery rates (FDR) to correct for multiple testing,⁶⁴ with an FDR ≤ 0.05 used as the threshold for significant PVE. In the analysis, we found that 11.3% of genes in AA and 8.3% of genes in EA have a PVE that significantly deviates from zero at FDR ≤ 0.05 . In AA, the median PVE is

24.6% across these significant genes (1,986 genes, mean = 26.67%; SD = 10.5%), with PVE estimates ranging from 8.49% to 79.46% (Figure S11A). In EA, the median PVE is 26.78% across these significant genes (1,440 genes, mean = 28.25%; SD = 9.88%), with PVE estimates ranging from 9.81% to 78.7% (Figure S11B). The PVE of tested common genes is generally consistent between AA and EA (Pearson's correlation = 0.57, p value < $2.23e-308$), and the PVE of common eGenes is also consistent between

A African American



B European American

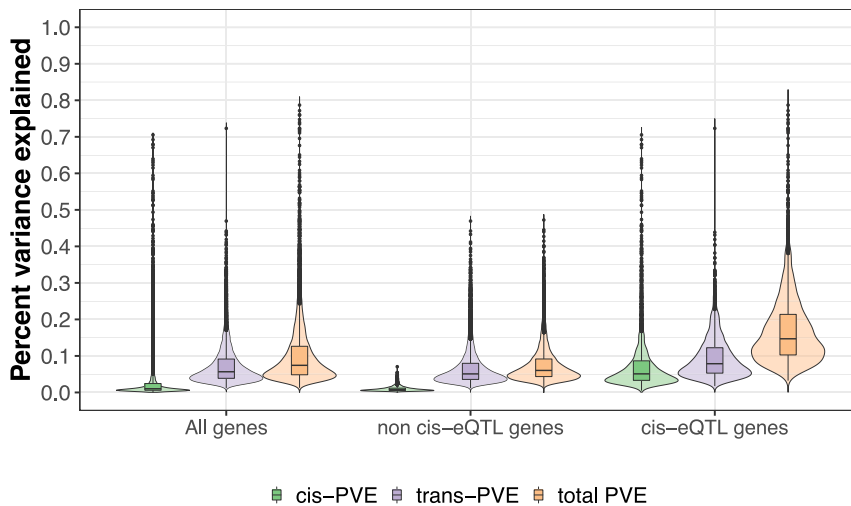


Figure 3. Estimation and Partitioning of SNP Heritability Underlying Gene Expression Variation in African Americans and European Americans

Proportion of variance (PVE; aka SNP heritability) in gene expression levels estimated for all genes (left three plots), genes without detectable eQTLs (middle three plots), and genes with detectable eQTLs (right three plots) in African Americans (A) and European Americans (B). PVE explained by all SNPs is referred to as total PVE (orange), which is partitioned into a component that is explained by *cis*-SNPs (*cis*-PVE; green) and another component that is explained by *trans*-SNPs (*trans*-PVE; purple). As expected, PVE in eGenes tends to be larger than that in non-eGenes or in all genes. The total PVE as well as the *cis*-PVE in *cis*-eQTL genes also tend to be larger than that in non-*cis*-eQTL genes or in all genes.

AA and EA (Pearson's correlation = 0.502, p value = $2.69e-194$) (Figures S12A and S12B). As one might expect, eGenes tend to have a higher PVE than non-eGenes (p value < $2.23e-308$) (Figures 3A and 3B): the median PVE is 14.19% across eGenes and 5.28% across non-eGenes in AA, and is 14.7% across eGenes and 6.03% across non-eGenes in EA.

With BSLMM, we partitioned the PVE of each gene into two parts: one that is explained by *cis*-SNPs and the other that is explained by *trans*-SNPs. Consistent with previous studies,¹⁴ we found that the majority of PVE is explained by *trans*-SNPs, with only a fraction explained by *cis*-SNPs: the median proportion of PVE explained by *cis*-SNPs is only 1.03% (mean = 3.09%; SD = 5.44%) across all genes in AA and is 1.01% (mean = 2.63%; SD = 4.85%) across all genes in EA. As one might expect, *cis*-SNPs explain a higher proportion of PVE in eGenes than in non-eGenes. Specifically, the median proportion of PVE explained by *cis*-SNPs is 5.36% (mean = 7.93%; SD = 7.76%) across eGenes in AA and is 5.09% (mean = 7.61%; SD = 7.63%)

across eGenes in EA. The proportion of PVE in eGenes explained by *cis*-SNPs is correlated between AA and EA (Pearson's correlation coefficient = 0.62, p value < $2.23e-308$), and the proportion of PVE in eGenes explained by *trans*-SNPs is also correlated between AA and EA (Pearson's correlation coefficient = 0.18, p value = $1.33e-22$). For most eGenes, the primary eQTLs is able to explain a large proportion of the total *cis*-PVE (the PVE explained by *cis*-SNPs) in both AA and EA populations (Figures S13 and S14): the primary eQTL explains a median of 64.52%

cis-PVE in AA and 80.43% in EA. Note that the heritability estimates obtained using *trans*-SNPs residing on different chromosomes are almost identical to those obtained using all *trans*-SNPs (Figure S15). In particular, the *cis* heritability estimates obtained from these two approaches are highly correlated (0.9988 or 0.9937 in AA and EA, respectively) and so are the *trans* heritability estimates (correlation = 0.9989 or 0.9933 in AA and EA, respectively).

Independent *cis*-eQTLs rRevealed through Conditional Analysis

Because the primary eQTL does not fully explain *cis*-PVE, we performed conditional analysis to identify additional independent eQTLs for eGenes (details in Material and Methods). Through conditional analysis, we identified 8,070 independent eQTLs in AA and 5,401 in EA (Table 4); these include 2,595 conditional eQTLs in AA and 999 conditional eQTLs in EA, in addition to the primary eQTLs identified earlier. We found that most eGenes have only one independent eQTL (i.e., primary eQTL), with the

Table 4. The Number of Independent eQTLs Identified in eGenes through the Conditional Analysis

	Number of Independent eQTLs								
	1	2	3	4	5	6	7	8	9
African American	3,725	1,203	368	104	49	14	7	4	1
European American	3,577	690	108	18	7	1	1	0	0

Table lists the number of eGenes in AA (first row) and EA (second row) that contain different number of independent eQTLs (columns).

proportion of eGenes with one eQTL lower in AA and higher in EA (68.03% in AA and 81.26% in EA; Fisher's exact test p value $< 2.23e-308$; Figures 4A and 4D). A substantial proportion of eGenes have two independent eQTLs, with the proportion higher in AA and lower in EA (21.97% in AA and 15.67% in EA; p value = $1.11e-15$). The remaining eGenes have three or more independent eQTLs and those eGenes are more likely to appear in AA than EA (9.99% in AA and 3.07% in EA; p value = $6.94e-45$). In addition, the eGenes in AA tend to have a higher number of independent eQTLs: the average number of eQTLs per eGene is 1.47 in AA and 1.23 in EA (Wilcoxon test p value = $2.04e-56$). The higher number of independent eQTLs for eGenes in AA may suggest a more complex gene regulatory mechanism in AA, although we also note that the higher number of independent eQTLs in AA may reflect in part the lower linkage disequilibrium among SNPs in AA and hence the higher statistical power in detecting conditional eQTLs in AA. By identifying conditional eQTLs, we can explain a higher proportion of total *cis*-PVE compared to that explained by primarily eQTLs only (Figures S13 and S14): both primary and conditional eQTL explains a median of 77.83% *cis*-PVE in AA and 86.28% in EA.

As one might expect,⁶⁵ the conditional eQTLs reside farther away from the TSS compared to the primary eQTLs, though they are still enriched around the TSS when compared with non-eQTLs (Figures 4C and 4F). The number of independent eQTLs across genes in the conditional analysis is positively correlated with the number of eSNPs in the unconditional analysis, more so in AA than in EA (Pearson's correlation coefficient = 0.41, p value = $3.34e-218$ in AA; correlation = 0.18, p value = $1.88e-22$ in EA); and positively correlated with the gene length, though to a much lesser extent (Spearman's correlation between \log_{10} transformed gene length and number of independent eQTLs = 0.08, p value = 0.57 in AA; correlation = 0.034, p value = 0.06 in EA; Figure S16). The number of independent eQTLs across eGenes is also positively correlated with the *cis*-PVE of each eGene, more so in AA than in EA (Pearson's correlation coefficient = 0.57, p value $< 2.23e-308$ in AA; correlation = 0.41, p value = $1.21e-123$ in EA; Figures 4B and 4E). The eGenes with more independent eQTLs are less conserved: the number of independent eQTLs across eGenes is positively correlated with the dN/dS scores (Pearson's correlation = 0.047, p value = $5e-04$ in AA; correlation = 0.001, p value = 0.94 in EA); and negatively correlated with the conserva-

tion score (phyloP score: Pearson's correlation coefficient = -0.082 , p value = $1.17e-11$ in AA; correlation = -0.11 , p value = $4.57e-09$ in EA; phastCons score: correlation = -0.078 , p value = $7.6e-09$ in AA; correlation = -0.086 , p value = $2.06e-06$ in EA).

Large Sample Size in GENOA Enables More Accurate Gene Expression Prediction

Finally, we illustrate how the large sample size in both AA and EA populations in GENOA can allow us to construct accurate gene expression prediction models, thus potentially facilitating powerful transcriptome-wide association analysis (TWAS).⁶⁶ To do so, we constructed gene expression prediction models for one gene at a time in AA and EA separately. Each prediction model uses all *cis*-SNPs as covariates and is constructed using BSLMM. Afterward, we evaluated the performance of these prediction models for the same gene in a separate eQTL mapping study, the Geuvadis study. The Geuvadis study consists of five different populations that include CEPH (CEU, $n = 92$), Finns (FIN, $n = 95$), British (GBR, $n = 96$), Toscani (TSI, $n = 93$), and Yoruba (YRI, $n = 89$). We evaluated the performance of the prediction models constructed in EA and AA separately in each of the five populations. In each analysis, we calculated the coefficients of determination (R^2) between the predicted gene expression and the observed gene expression to measure prediction performance.⁶⁶ As expected,⁶⁷ we found that genes with high heritability tend to be predicted with high accuracy. For example, the prediction R^2 achieved using GENOA AA samples is positively correlated with PVE across all genes, in each of the five populations in Geuvadis (mean correlation across five populations = 0.36, SD = 0.02; p value $< 2.23e-308$); similar patterns were observed with the model constructed based on GENOA EA samples (Figure S17). Also as expected,¹⁴ we found that the expression prediction models constructed in a population often perform well in the population of the same ancestry. For example, the prediction models based on EA performed better for predicting expression levels in FIN and CEU than in other populations (Tables S26 and S27), while the models constructed based on AA performed better in YRI than in other populations (Figure 5A and Table S23). The better performance of AA models in YRI highlights the need for eQTL mapping studies in the African American population.

Besides GENOA, we also obtained previously constructed gene expression prediction models using elastic net in the MESA study and evaluated their prediction performance

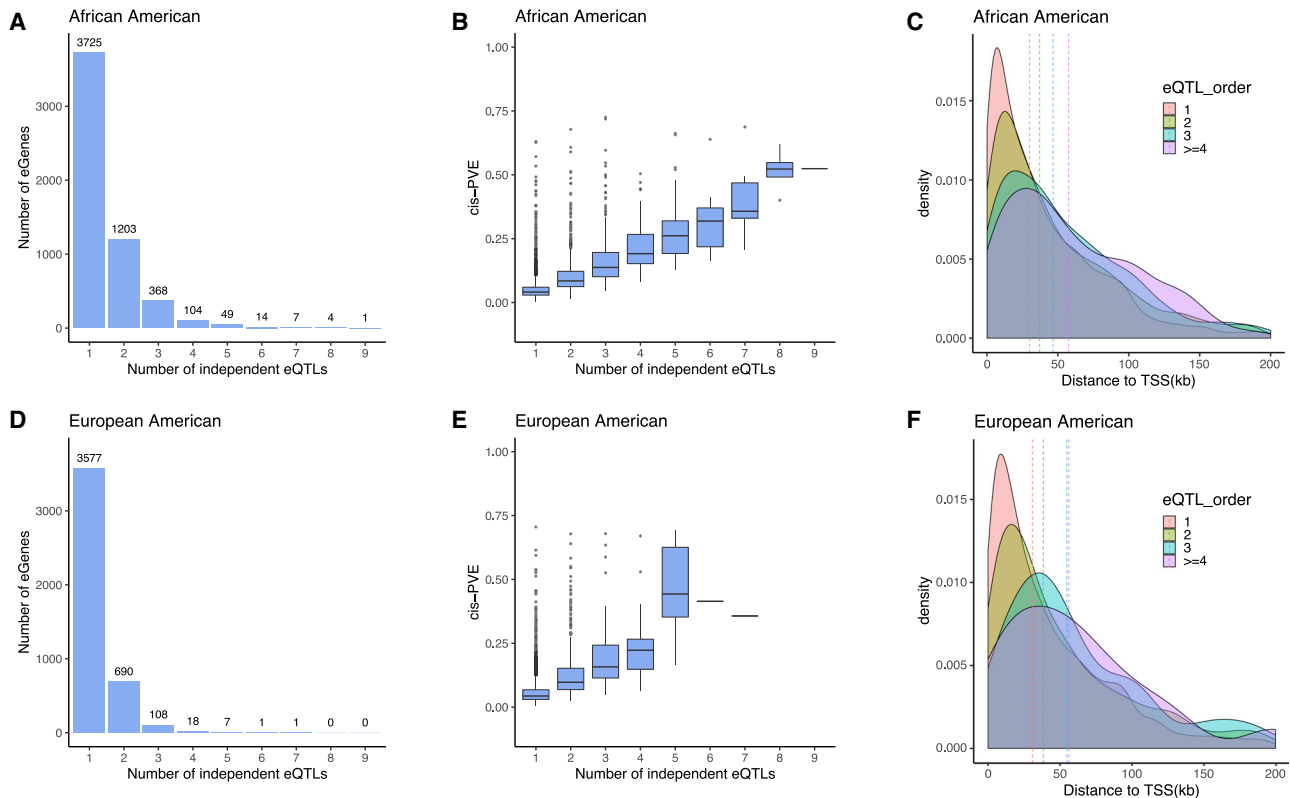


Figure 4. Characterization of the Conditional eQTLs

(A and D) Histogram shows the number of eGenes (y axis) that harbor different numbers of independent eQTLs (x axis) in African Americans (A) or European Americans (D). We displayed eGenes that harbor up to nine independent eQTLs, with the detailed number of eQTLs listed above each bar. A large fraction of eGenes harbor a small number of independent eQTLs.

(B and E) The proportion of variance (PVE) in gene expression levels explained by SNPs are higher for eGenes that harbor a larger number of independent eQTLs in African Americans (B) or European Americans (E).

(C and F) Density plot shows the distance from eQTL to the transcription start site (TSS) of the corresponding eGene. The density plot is stratified by the number of eQTLs: eGenes with one independent eQTL is colored in red; eGenes with two independent eQTL is colored in green; eGenes with three independent eQTL is colored in blue; eGenes with four or more independent eQTL is colored in purple. Dashed lines represent the median distance between eQTL and TSS in the four stratified groups in African Americans (C) or European Americans (F).

in Geuvadis. The MESA study consists of three populations: African American (AFA, $n = 233$), Hispanic (HIS, $n = 352$), and European (CAU, $n = 578$). For a fair comparison, we also constructed gene expression prediction models using elastic net in GENOA, in addition to using BSLMM above. In the analysis, we found that the gene prediction models constructed based on GENOA AA or EA samples outperform those constructed based on the MESA AFA, CAU, or HIS (Tables S23–S27). For example, for predicting gene expression in YRI, models constructed based on AA in GENOA with elastic net achieve a prediction R^2 above 0.1 in 337 genes, which represents a 75.5% gain compared to the prediction models constructed based on the AFA population in MESA with elastic net (Table S23). Similarly, for predicting gene expression in GBR, models constructed based on EA in GENOA with elastic net achieve a prediction R^2 above 0.1 in 415 genes, which represents a 30.1% gain compared to the prediction models constructed based on the CAU population in MESA with elastic net (Table S24).

The accurate expression prediction performance based on GENOA also translates to a high power for TWAS anal-

ysis.⁶⁶ To illustrate the TWAS power gain brought by GENOA, we applied the prediction models constructed in each of the five populations (GENOA: AA and EA; MESA: AFA, HIS, and CAU) to seven common diseases collected from a GWAS case control study: the WTCCC.⁵⁵ These seven diseases include Crohn disease (CD), rheumatoid arthritis (RA), bipolar disorder (BD), type 2 diabetes (T2D), coronary artery disease (CAD), and hypertension (HT). For each gene and disease pair in turn, we tested for the association between the predicted gene expression and disease status using logistic regression, with the first ten genetic PCs included as covariates. Overall, we found that models constructed based on GENOA identified more associations with the seven common diseases compared to models constructed based on MESA (Figures 5C–5H and S18 and Table S28). For example, using elastic net for constructing the gene prediction models in GENOA AA, we identified a total of 48 genes in WTCCC, among which 42 are reported to be associated with the same trait in the GeneCards database.⁵⁷ Using the same elastic net for constructing the gene prediction models in MESA AFA, we

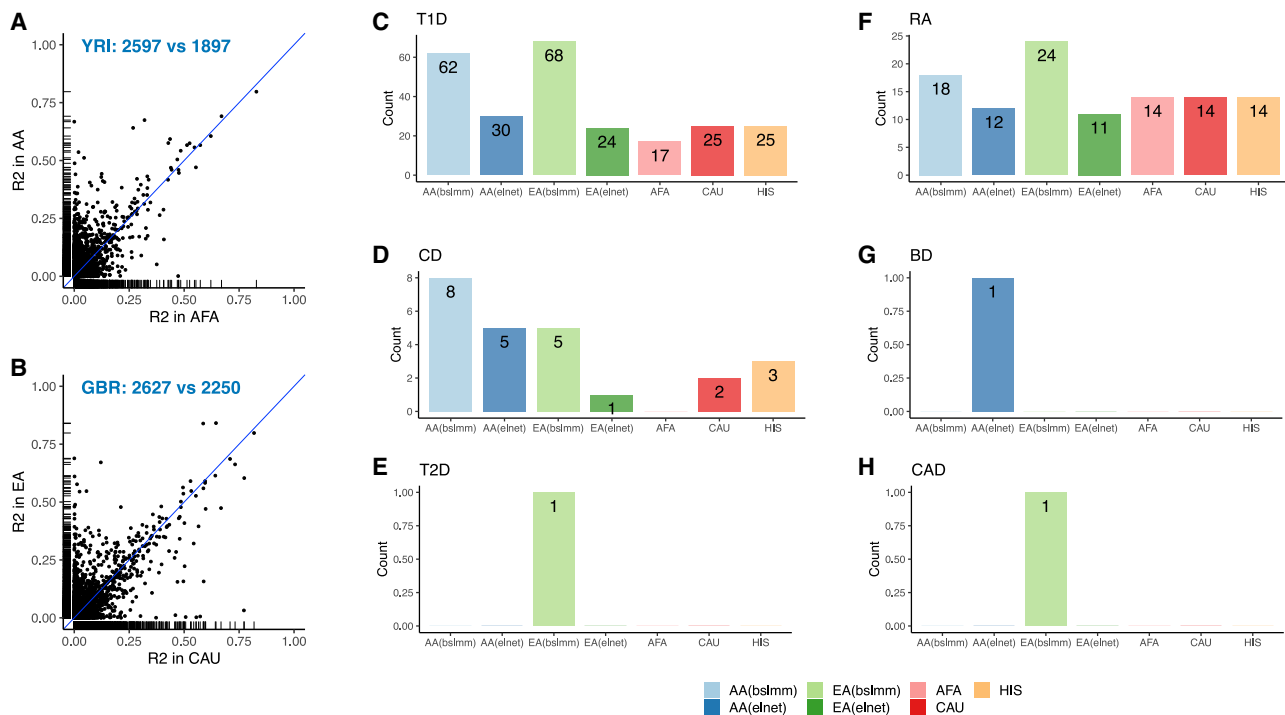


Figure 5. Application of GENOA eQTL Mapping Results in Gene Expression Prediction and TWAS in WTCCC

(A) Comparison of the prediction performance measured by R^2 using GENOA AA (y axis) and MESA AFA (x axis) eQTL mapping results for the Geuvadis YRI data. The panel also lists the number of genes where AA performs better (2,597) and the number of genes where AA performs worse than AFA (1,897). Here we compare the commonly predicted genes between AA and AFA.

(B) Comparison of the prediction performance measured by R^2 using GENOA EA (y axis) and MESA CAU (x axis) eQTL mapping results for the Geuvadis GBR data. The panel also lists the number of genes where EA performs better (2,627) and the number of genes where EA performs worse (2,250) than CAU. Here we compare the commonly predicted genes between EA and CAU.

(C–H) Barplots display the number of significant genes from TWAS analysis using gene expression models constructed based on different populations. The significant genes are those passing the genome-wide significance threshold via Bonferroni correction ($\alpha = 0.05/\text{number of genes tested}$) in each of the seven common diseases in WTCCC that include Crohn disease (CD), rheumatoid arthritis (RA), bipolar disorder (BD), type 1 diabetes (T1D), type 2 diabetes (T2D), coronary artery disease (CAD), and hypertension (HT). The result for HT is not shown since no gene was identified in any population. The five populations used to construct the gene expression models include GENOA AA BSLMM (light blue), AA elastic net (deep blue), GENOA EA BSLMM (light green), GENOA EA elastic net (deep green), MESA AFA (pink), MESA CAU (red), and MESA HIS (yellow).

identified a total of 40 genes in WTCCC, among which 37 are reported in the GeneCards. Table S29 lists the significant genes identified by TWAS analysis using GENOA AA samples, the majority of which have also been identified in much larger-scale GWASs.^{68–70}

Discussion

We have presented a comprehensive eQTL mapping analysis in GENOA. Our study is a large eQTL mapping study performed in the African American population. The large AA sample size in GENOA allows us to identify a substantial number of eQTLs and eGenes in AA, many of which were not identified in previous AA eQTL mapping studies.⁸ In addition, we identified a higher number of eGenes in AA than in EA, likely due to the larger sample size, higher number of *cis*-SNPs per gene, and/or potentially higher diversity in AA. Importantly, only a small percentage of the significant gene-SNP pairs identified in AA are also identified in EA, highlighting the importance of

eQTL mapping with AA samples. The large AA sample size also allows us to construct accurate gene expression prediction models in the African American population, facilitating powerful TWAS analysis there. These analyses and results enhance our understanding of the genetic architecture underlying gene expression variation and facilitate the future investigation of the causal molecular mechanisms underlying common diseases and disease-related complex traits.

The availability of both large-scale AA and EA samples in GENOA allows us to perform comparisons between these two populations. We found that eGenes with multiple independent eQTLs are often less conserved and eGenes shared between AA and EA are also less conserved. Indeed, eGenes are depleted from genes with crucial roles in regulating cell functions.⁶⁵ The comparison results highlight the importance of negative selection, which constrains biologically important regions, removes large-effect regulatory variants, and reshapes the genetic architecture.³⁶ Through comparison, we found that substantial differences exist between the two populations of

AA and EA. Specifically, despite the similar sample sizes between AA and EA, we identified a higher number of independent eQTLs in AA than in EA through conditional analysis. A higher number of independent eQTLs in AA supports the potentially more complex regulatory mechanisms underlying gene expression in AA. While the identified eQTLs vary across populations, the shared eQTLs in the AA and EA populations nevertheless often share similar effect sizes and effect directions. In addition, the gene expression prediction models constructed based on AA apply reasonably accurately for gene expression prediction in EA, and vice versa. Therefore, at least part of the eQTL mapping results from one population can be transferred to the other populations.¹² Further integrating the GENOA study with other previous studies for joint eQTL mapping or joint TWAS analysis is an important direction for future exploration.

Finally, while we have identified many primary eQTLs in the main analysis, we acknowledge that the identified primary eQTLs do not explain all *cis*-SNP heritability in eGenes (median = 64.52% in AA and 80.43% in EA). We can identify many additional eQTLs through conditional analysis. However, these conditional eQTLs in addition to the primary eQTLs again cannot explain all *cis*-SNP heritability (median = 77.83% AA and 86.28% in EA). In addition, the *cis*-SNP heritability only represents a small proportion of total SNP heritability, suggesting that a large fraction of SNP heritability remains largely unidentified. The incomplete *cis*-heritability explained by identified eQTLs support the likely polygenic architecture underlying gene expression variation. Therefore, future studies with larger sample sizes are necessary to fully capture the genetic architecture underlying gene expression variation.

Accession Numbers

The accession numbers for the gene expression data used in this analysis are Gene Expression Omnibus (GEO): GSE138914 for AA and GSE49531 for EA. The accession number for the SNP data used in this analysis is Database of Genotypes and Phenotypes (dbGaP): phs001238.v2.p1. Due to IRB restriction, mapping of the sample IDs between genotype data (dbGaP) and gene expression data (GEO) cannot be provided publicly but are available upon written request to JS and SK.

Supplemental Data

Supplemental Data can be found online at <https://doi.org/10.1016/j.ajhg.2020.03.002>.

Acknowledgments

Support for the Genetic Epidemiology Network of Arteriopathy (GENOA) data collection and analysis was provided by the National Heart, Lung and Blood Institute (HL054457, HL100185, HL119443, and HL133221) and the National Institute of Neurological Disorders and Stroke (NS041558) of the National Institutes

of Health. This study was also partially supported by the National Human Genome Research Institutes grant R01HG009124 and National Science Foundation grant DMS1712933. The funders had no role in study design, data collection and analysis, decision to publish, or preparation of the manuscript.

Declaration of Interests

The authors declare no competing interests.

Received: October 6, 2019

Accepted: March 6, 2020

Published: March 26, 2020

Web Resources

Brainarray, <http://brainarray.mbni.med.umich.edu/Brainarray/Database/CustomCDF>
FRANC interface, <http://web.cbio.uct.ac.za/ITGOM/franc/>
GEMMA, <https://www.xzlab.org/software.html>
Geuvadis eQTL mapping results, <http://jungle.unige.ch/~lappalainen/geuvadis/>
MESA *cis*-SNP weights, https://github.com/WheelerLab/DivPop/tree/master/unfiltered_dbs
MESA eQTL mapping results, <https://www.dropbox.com/sh/f6un5evevvy19/AAA3sfa1DgqY67tx4q36P341a?dl=0>
OMIM, <https://www.omim.org/>
Zhou lab: summary statistics from eQTL mapping analysis along with all analysis scripts, <http://www.xzlab.org/data.html>

References

1. Nica, A.C., Montgomery, S.B., Dimas, A.S., Stranger, B.E., Beazley, C., Barroso, I., and Dermitzakis, E.T. (2010). Candidate causal regulatory effects by integration of expression QTLs with complex trait genetic associations. *PLoS Genet.* *6*, e1000895.
2. Gusev, A., Lee, S.H., Trynka, G., Finucane, H., Vilhjálmsson, B.J., Xu, H., Zang, C., Ripke, S., Bulik-Sullivan, B., Stahl, E., et al.; Schizophrenia Working Group of the Psychiatric Genomics Consortium; SWE-SCZ Consortium; Schizophrenia Working Group of the Psychiatric Genomics Consortium; and SWE-SCZ Consortium (2014). Partitioning heritability of regulatory and cell-type-specific variants across 11 common diseases. *Am. J. Hum. Genet.* *95*, 535–552.
3. Torres, J.M., Gamazon, E.R., Parra, E.J., Below, J.E., Valladares-Salgado, A., Wachter, N., Cruz, M., Hanis, C.L., and Cox, N.J. (2014). Cross-tissue and tissue-specific eQTLs: partitioning the heritability of a complex trait. *Am. J. Hum. Genet.* *95*, 521–534.
4. Li, Y.I., van de Geijn, B., Raj, A., Knowles, D.A., Petti, A.A., Golani, D., Gilad, Y., and Pritchard, J.K. (2016). RNA splicing is a primary link between genetic variation and disease. *Science* *352*, 600–604.
5. Schadt, E.E., Monks, S.A., Drake, T.A., Lusk, A.J., Che, N., Colinao, V., Ruff, T.G., Milligan, S.B., Lamb, J.R., Cavet, G., et al. (2003). Genetics of gene expression surveyed in maize, mouse and man. *Nature* *422*, 297–302.
6. Morley, M., Molony, C.M., Weber, T.M., Devlin, J.L., Ewens, K.G., Spielman, R.S., and Cheung, V.G. (2004). Genetic analysis of genome-wide variation in human gene expression. *Nature* *430*, 743–747.

7. Battle, A., Mostafavi, S., Zhu, X., Potash, J.B., Weissman, M.M., McCormick, C., Haudenschild, C.D., Beckman, K.B., Shi, J., Mei, R., et al. (2014). Characterizing the genetic basis of transcriptome diversity through RNA-sequencing of 922 individuals. *Genome Res.* 24, 14–24.
8. Lappalainen, T., Sammeth, M., Friedländer, M.R., 't Hoen, P.A.C., Monlong, J., Rivas, M.A., González-Porta, M., Kurbatova, N., Griebel, T., Ferreira, P.G., et al.; Geuvadis Consortium (2013). Transcriptome and genome sequencing uncovers functional variation in humans. *Nature* 501, 506–511.
9. Emilsson, V., Thorleifsson, G., Zhang, B., Leonardson, A.S., Zink, F., Zhu, J., Carlson, S., Helgason, A., Walters, G.B., Gunnarsdottir, S., et al. (2008). Genetics of gene expression and its effect on disease. *Nature* 452, 423–428.
10. Nicolae, D.L., Gamazon, E., Zhang, W., Duan, S., Dolan, M.E., and Cox, N.J. (2010). Trait-associated SNPs are more likely to be eQTLs: annotation to enhance discovery from GWAS. *PLoS Genet.* 6, e1000888.
11. Hao, X., Zeng, P., Zhang, S., and Zhou, X. (2018). Identifying and exploiting trait-relevant tissues with multiple functional annotations in genome-wide association studies. *PLoS Genet.* 14, e1007186.
12. Stranger, B.E., Montgomery, S.B., Dimas, A.S., Parts, L., Stegle, O., Ingle, C.E., Sekowska, M., Smith, G.D., Evans, D., Gutierrez-Arcelus, M., et al. (2012). Patterns of cis regulatory variation in diverse human populations. *PLoS Genet.* 8, e1002639.
13. Quach, H., Rotival, M., Pothlichet, J., Loh, Y.E., Dannemann, M., Zidane, N., Laval, G., Patin, E., Harmant, C., Lopez, M., et al. (2016). Genetic Adaptation and Neandertal Admixture Shaped the Immune System of Human Populations. *Cell* 167, 643–656.e17.
14. Mogil, L.S., Andaleon, A., Badalamenti, A., Dickinson, S.P., Guo, X., Rotter, J.L., Johnson, W.C., Im, H.K., Liu, Y., and Wheeler, H.E. (2018). Genetic architecture of gene expression traits across diverse populations. *PLoS Genet.* 14, e1007586.
15. Kelly, D.E., Hansen, M.E.B., and Tishkoff, S.A. (2017). Global variation in gene expression and the value of diverse sampling. *Curr. Opin. Syst. Biol.* 1, 102–108.
16. Stranger, B.E., Nica, A.C., Forrest, M.S., Dimas, A., Bird, C.P., Beazley, C., Ingle, C.E., Dunning, M., Flicek, P., Koller, D., et al. (2007). Population genomics of human gene expression. *Nat. Genet.* 39, 1217–1224.
17. Spielman, R.S., Bastone, L.A., Burdick, J.T., Morley, M., Ewens, W.J., and Cheung, V.G. (2007). Common genetic variants account for differences in gene expression among ethnic groups. *Nat. Genet.* 39, 226–231.
18. Daniels, P.R., Kardia, S.L.R., Hanis, C.L., Brown, C.A., Hutchinson, R., Boerwinkle, E., Turner, S.T.; and Genetic Epidemiology Network of Arteriopathy study (2004). Familial aggregation of hypertension treatment and control in the Genetic Epidemiology Network of Arteriopathy (GENOA) study. *Am. J. Med.* 116, 676–681.
19. Delaneau, O., Zagury, J.F., and Marchini, J. (2013). Improved whole-chromosome phasing for disease and population genetic studies. *Nat. Methods* 10, 5–6.
20. Howie, B.N., Donnelly, P., and Marchini, J. (2009). A flexible and accurate genotype imputation method for the next generation of genome-wide association studies. *PLoS Genet.* 5, e1000529.
21. Conomos, M.P., Reiner, A.P., Weir, B.S., and Thornton, T.A. (2016). Model-free Estimation of Recent Genetic Relatedness. *Am. J. Hum. Genet.* 98, 127–148.
22. Zhou, X., and Stephens, M. (2012). Genome-wide efficient mixed-model analysis for association studies. *Nat. Genet.* 44, 821–824.
23. Ackermann, M., Sikora-Wohlfeld, W., and Beyer, A. (2013). Impact of natural genetic variation on gene expression dynamics. *PLoS Genet.* 9, e1003514.
24. Gerrits, A., Li, Y., Tesson, B.M., Bystrykh, L.V., Weersing, E., Ausema, A., Dontje, B., Wang, X., Breitling, R., Jansen, R.C., and de Haan, G. (2009). Expression quantitative trait loci are highly sensitive to cellular differentiation state. *PLoS Genet.* 5, e1000692.
25. Lockstone, H.E. (2011). Exon array data analysis using Affymetrix power tools and R statistical software. *Brief. Bioinform.* 12, 634–644.
26. Irizarry, R.A., Bolstad, B.M., Collin, F., Cope, L.M., Hobbs, B., and Speed, T.P. (2003). Summaries of Affymetrix GeneChip probe level data. *Nucleic Acids Res.* 31, e15.
27. Dai, M., Wang, P., Boyd, A.D., Kostov, G., Athey, B., Jones, E.G., Bunney, W.E., Myers, R.M., Speed, T.P., Akil, H., et al. (2005). Evolving gene/transcript definitions significantly alter the interpretation of GeneChip data. *Nucleic Acids Res.* 33, e175–e175.
28. Saha, A., and Battle, A. (2018). False positives in trans-eQTL and co-expression analyses arising from RNA-sequencing alignment errors. *F1000Res.* 7, 1860.
29. Johnson, W.E., Li, C., and Rabinovic, A. (2007). Adjusting batch effects in microarray expression data using empirical Bayes methods. *Biostatistics* 8, 118–127.
30. Peters, J.E., Lyons, P.A., Lee, J.C., Richard, A.C., Fortune, M.D., Newcombe, P.J., Richardson, S., and Smith, K.G.C. (2016). Insight into Genotype-Phenotype Associations through eQTL Mapping in Multiple Cell Types in Health and Immune-Mediated Disease. *PLoS Genet.* 12, e1005908.
31. Barreiro, L.B., Tailleux, L., Pai, A.A., Gicquel, B., Marioni, J.C., and Gilad, Y. (2012). Deciphering the genetic architecture of variation in the immune response to Mycobacterium tuberculosis infection. *Proc. Natl. Acad. Sci. USA* 109, 1204–1209.
32. Pickrell, J.K., Marioni, J.C., Pai, A.A., Degner, J.F., Engelhardt, B.E., Nkadori, E., Veyrieras, J.B., Stephens, M., Gilad, Y., and Pritchard, J.K. (2010). Understanding mechanisms underlying human gene expression variation with RNA sequencing. *Nature* 464, 768–772.
33. Jansen, R., Hottenga, J.J., Nivard, M.G., Abdellaoui, A., Laport, B., de Geus, E.J., Wright, F.A., Penninx, B.W.J.H., and Boomsma, D.I. (2017). Conditional eQTL analysis reveals allelic heterogeneity of gene expression. *Hum. Mol. Genet.* 26, 1444–1451.
34. Chang, C.C., Chow, C.C., Tellier, L.C., Vattikuti, S., Purcell, S.M., and Lee, J.J. (2015). Second-generation PLINK: rising to the challenge of larger and richer datasets. *Gigascience* 4, 7.
35. Holsinger, K.E., and Weir, B.S. (2009). Genetics in geographically structured populations: defining, estimating and interpreting F(ST). *Nat. Rev. Genet.* 10, 639–650.
36. Battle, A., Brown, C.D., Engelhardt, B.E., Montgomery, S.B.; GTEx Consortium; Laboratory, Data Analysis & Coordinating Center (LDACC)—Analysis Working Group; Statistical Methods groups—Analysis Working Group; Enhancing GTEx (eGTEx) groups; NIH Common Fund; NIH/NCI; NIH/NHGRI; NIH/NIMH; NIH/NIDA; Biospecimen Collection Source Site—NDRI; Biospecimen Collection Source Site—RPCI; Biospecimen Core Resource—VARI; Brain Bank Repository—University of Miami Brain Endowment Bank; Leidos Biomedical—Project Management; ELSI Study; Genome Browser Data Integration

- &Visualization—EBI; Genome Browser Data Integration &Visualization—UCSC Genomics Institute, University of California Santa Cruz; Lead analysts; Laboratory, Data Analysis &Coordinating Center (LDACC); NIH program management; Biospecimen collection; Pathology; and eQTL manuscript working group (2017). Genetic effects on gene expression across human tissues. *Nature* 550, 204–213.
37. Storey, J.D., and Tibshirani, R. (2003). Statistical significance for genomewide studies. *Proc. Natl. Acad. Sci. USA* 100, 9440–9445.
 38. Guan, Y. (2014). Detecting structure of haplotypes and local ancestry. *Genetics* 196, 625–642.
 39. Zhong, Y., Perera, M.A., and Gamazon, E.R. (2019). On Using Local Ancestry to Characterize the Genetic Architecture of Human Traits: Genetic Regulation of Gene Expression in Multiethnic or Admixed Populations. *Am. J. Hum. Genet.* 104, 1097–1115.
 40. Zhou, X., Carbonetto, P., and Stephens, M. (2013). Polygenic modeling with bayesian sparse linear mixed models. *PLoS Genet.* 9, e1003264.
 41. Pollard, K.S., Hubisz, M.J., Rosenbloom, K.R., and Siepel, A. (2010). Detection of nonneutral substitution rates on mammalian phylogenies. *Genome Res.* 20, 110–121.
 42. Siepel, A., Bejerano, G., Pedersen, J.S., Hinrichs, A.S., Hou, M., Rosenbloom, K., Clawson, H., Spieth, J., Hillier, L.W., Richards, S., et al. (2005). Evolutionarily conserved elements in vertebrate, insect, worm, and yeast genomes. *Genome Res.* 15, 1034–1050.
 43. Kryazhimskiy, S., and Plotkin, J.B. (2008). The population genetics of dN/dS. *PLoS Genet.* 4, e1000304.
 44. Siepel, A., Pollard, K.S., and Haussler, D. (2006). New methods for detecting lineage-specific selection. *Lect N Bioinform* 3909, 190–205.
 45. Li, W.H., Wu, C.I., and Luo, C.C. (1985). A new method for estimating synonymous and nonsynonymous rates of nucleotide substitution considering the relative likelihood of nucleotide and codon changes. *Mol. Biol. Evol.* 2, 150–174.
 46. Kent, W.J., Sugnet, C.W., Furey, T.S., Roskin, K.M., Pringle, T.H., Zahler, A.M., and Haussler, D. (2002). The human genome browser at UCSC. *Genome Res.* 12, 996–1006.
 47. Durinck, S., Moreau, Y., Kasprzyk, A., Davis, S., De Moor, B., Brazma, A., and Huber, W. (2005). BioMart and Bioconductor: a powerful link between biological databases and microarray data analysis. *Bioinformatics* 21, 3439–3440.
 48. Raudvere, U., Kolberg, L., Kuzmin, I., Arak, T., Adler, P., Peterson, H., and Vilo, J. (2019). g:Profiler: a web server for functional enrichment analysis and conversions of gene lists (2019 update). *Nucleic Acids Res.* 47 (W1), W191–W198.
 49. Prüfer, K., Muetzel, B., Do, H.H., Weiss, G., Khaitovich, P., Rahm, E., Pääbo, S., Lachmann, M., and Enard, W. (2007). FUNC: a package for detecting significant associations between gene sets and ontological annotations. *BMC Bioinformatics* 8, 41.
 50. Ashburner, M., Ball, C.A., Blake, J.A., Botstein, D., Butler, H., Cherry, J.M., Davis, A.P., Dolinski, K., Dwight, S.S., Eppig, J.T., et al.; The Gene Ontology Consortium (2000). Gene ontology: tool for the unification of biology. *Nat. Genet.* 25, 25–29.
 51. Friedman, J., Hastie, T., and Tibshirani, R. (2010). Regularization Paths for Generalized Linear Models via Coordinate Descent. *J. Stat. Softw.* 33, 1–22.
 52. Harrow, J., Frankish, A., Gonzalez, J.M., Tapanari, E., Diekhans, M., Kokocinski, F., Aken, B.L., Barrell, D., Zadissa, A., Searle, S., et al. (2012). GENCODE: the reference human genome annotation for The ENCODE Project. *Genome Res.* 22, 1760–1774.
 53. Stegle, O., Parts, L., Piipari, M., Winn, J., and Durbin, R. (2012). Using probabilistic estimation of expression residuals (PEER) to obtain increased power and interpretability of gene expression analyses. *Nat. Protoc.* 7, 500–507.
 54. Mikhaylova, A.V., and Thornton, T.A. (2019). Accuracy of Gene Expression Prediction From Genotype Data With PrediXcan Varies Across and Within Continental Populations. *Front. Genet.* 10, 261.
 55. Wellcome Trust Case Control, C.; and Wellcome Trust Case Control Consortium (2007). Genome-wide association study of 14,000 cases of seven common diseases and 3,000 shared controls. *Nature* 447, 661–678.
 56. Guan, Y., and Stephens, M. (2008). Practical issues in imputation-based association mapping. *PLoS Genet.* 4, e1000279.
 57. Safran, M., Chalifa-Caspi, V., Shmueli, O., Olender, T., Lapidot, M., Rosen, N., Shmoish, M., Peter, Y., Glusman, G., Feldmesser, E., et al. (2003). Human Gene-Centric Databases at the Weizmann Institute of Science: GeneCards, UDB, CroW 21 and HORDE. *Nucleic Acids Res.* 31, 142–146.
 58. Aguiar, V.R.C., César, J., Delaneau, O., Dermitzakis, E.T., and Meyer, D. (2019). Expression estimation and eQTL mapping for HLA genes with a personalized pipeline. *PLoS Genet.* 15, e1008091.
 59. Tung, J., Zhou, X., Alberts, S.C., Stephens, M., and Gilad, Y. (2015). The genetic architecture of gene expression levels in wild baboons. *eLife* 4, e04729.
 60. Veyrieras, J.B., Kudravalli, S., Kim, S.Y., Dermitzakis, E.T., Gilad, Y., Stephens, M., and Pritchard, J.K. (2008). High-resolution mapping of expression-QTLs yields insight into human gene regulation. *PLoS Genet.* 4, e1000214.
 61. Glassberg, E.C., Gao, Z., Harpak, A., Lan, X., and Pritchard, J.K. (2019). Evidence for Weak Selective Constraint on Human Gene Expression. *Genetics* 211, 757–772.
 62. Blekhman, R., Man, O., Herrmann, L., Boyko, A.R., Indap, A., Kosiol, C., Bustamante, C.D., Teshima, K.M., and Przeworski, M. (2008). Natural selection on genes that underlie human disease susceptibility. *Curr. Biol.* 18, 883–889.
 63. Gershoni, M., and Petrokovski, S. (2014). Reduced selection and accumulation of deleterious mutations in genes exclusively expressed in men. *Nat. Commun.* 5, 4438.
 64. Benjamini, Y., Drai, D., Elmer, G., Kafkafi, N., and Golani, I. (2001). Controlling the false discovery rate in behavior genetics research. *Behav. Brain Res.* 125, 279–284.
 65. Dobbyn, A., Huckins, L.M., Boocock, J., Sloofman, L.G., Glicksberg, B.S., Giambartolomei, C., Hoffman, G.E., Perumal, T.M., Girdhar, K., Jiang, Y., et al.; CommonMind Consortium (2018). Landscape of Conditional eQTL in Dorsolateral Prefrontal Cortex and Co-localization with Schizophrenia GWAS. *Am. J. Hum. Genet.* 102, 1169–1184.
 66. Zeng, P., and Zhou, X. (2017). Non-parametric genetic prediction of complex traits with latent Dirichlet process regression models. *Nat. Commun.* 8, 456.
 67. Wheeler, H.E., Shah, K.P., Brenner, J., Garcia, T., Aquino-Michaels, K., Cox, N.J., Nicolae, D.L., Im, H.K.; and GTEx Consortium (2016). Survey of the Heritability and Sparse Architecture of Gene Expression Traits across Human Tissues. *PLoS Genet.* 12, e1006423.
 68. Gonzalez, S., Gupta, J., Villa, E., Mallawaarachchi, I., Rodriguez, M., Ramirez, M., Zavala, J., Armas, R., Dassori, A.,

- Contreras, J., et al. (2016). Replication of genome-wide association study (GWAS) susceptibility loci in a Latino bipolar disorder cohort. *Bipolar Disord.* *18*, 520–527.
69. Sanjak, J.S., Long, A.D., and Thornton, K.R. (2016). Efficient Software for Multi-marker, Region-Based Analysis of GWAS Data. *G3 (Bethesda)* *6*, 1023–1030.
70. Zanetti, D., Via, M., Carreras-Torres, R., Esteban, E., Chaabani, H., Anaibar, F., Harich, N., Habbal, R., Ghalim, N., and Moral, P. (2016). Analysis of Genomic Regions Associated With Coronary Artery Disease Reveals Continent-Specific Single Nucleotide Polymorphisms in North African Populations. *J. Epidemiol.* *26*, 264–271.

The American Journal of Human Genetics, Volume 106

Supplemental Data

Genetic Architecture of Gene Expression

in European and African Americans:

An eQTL Mapping Study in GENOA

Lulu Shang, Jennifer A. Smith, Wei Zhao, Minjung Kho, Stephen T. Turner, Thomas H. Mosley, Sharon L.R. Kardia, and Xiang Zhou

Supplemental Data:

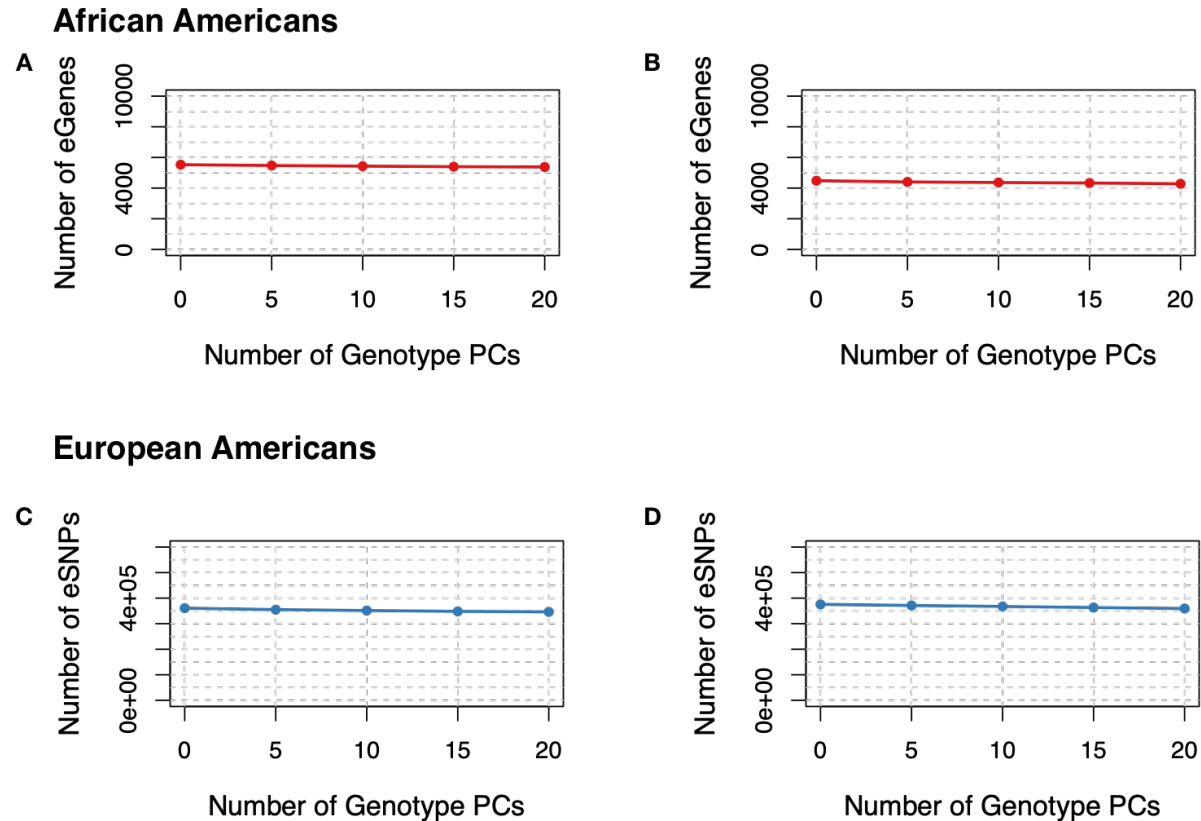


Figure S1. Number of eGenes and eSNPs identified is stable with respect to the number of genotype PCs included in the model. Number of eGenes (A, C) (in red) and eSNPs (B, D) (in blue) identified with respect to the number of genotype principal components (PCs) included in the model (x-axis) in African Americans (A, B) and European Americans (C, D). Significance is based on 5% false discovery rate (FDR). The number of genotype PCs varied from 0 to 20. In the analysis, we used the GENESIS package in R to infer population structure and estimate individual relatedness. We used the PC-AiR function to extract the genotype PCs and used PC-Relate to estimate an individual relatedness matrix after adjusting for these PCs. Both PCs and the relatedness matrix were included as covariates in the eQTL mapping analysis. The number of discoveries is stable with respect to the number of genotype PCs included in the model.

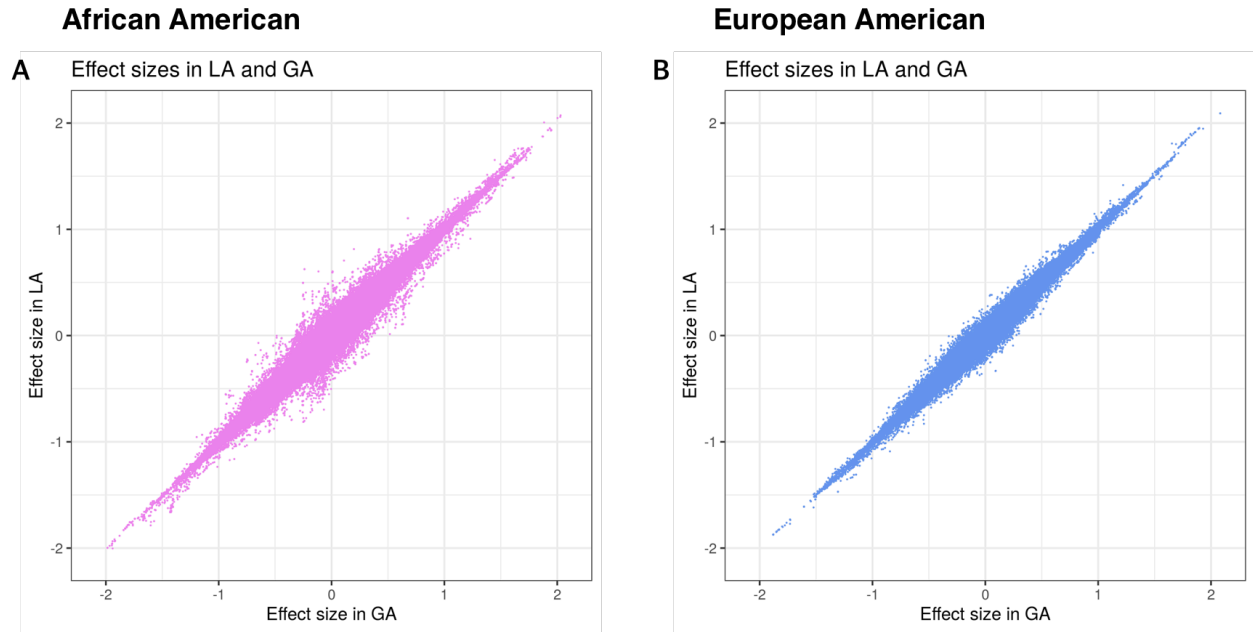


Figure S2. Effect sizes comparison for gene-SNP pairs adjusting for Local Ancestry (LA) and Global Ancestry (GA) in the African American samples and European American samples. The estimated effect size of gene-SNP pairs adjusting for global ancestry (x-axis) is positively correlated with the estimated effect size of gene-SNP pairs adjusting for local ancestry (y-axis) in African Americans (**A**) and European Americans (**B**).

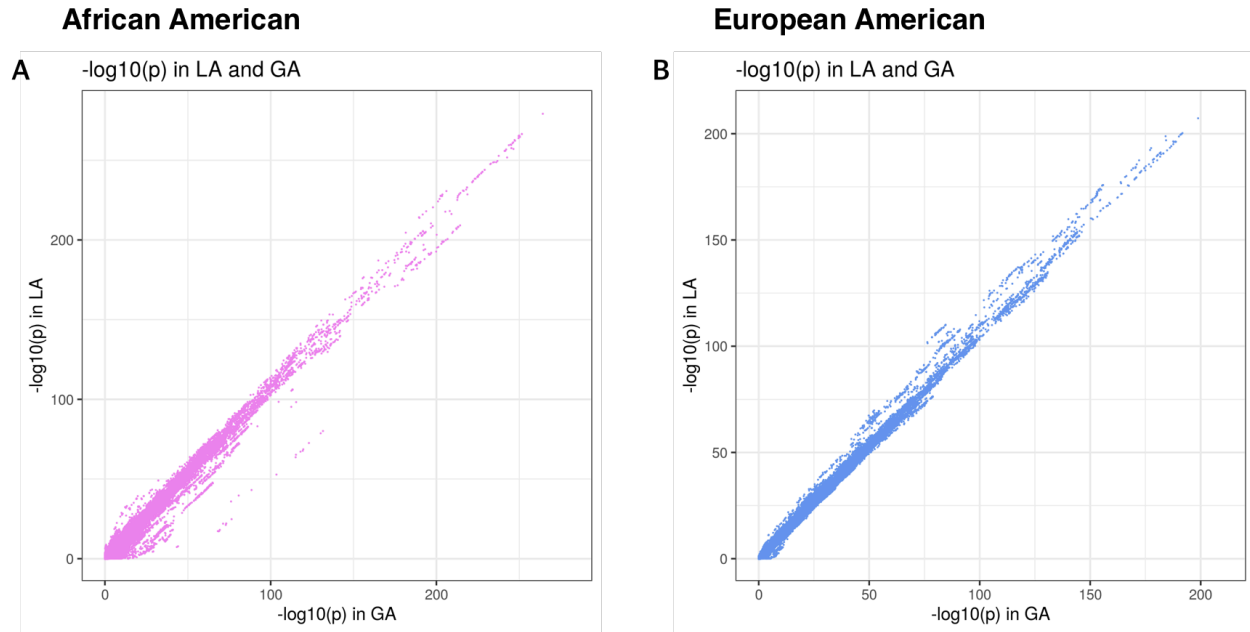


Figure S3. $-\log_{10}(p)$ comparison for gene-SNP pairs adjusting for Local Ancestry (LA) and Global Ancestry (GA) in the African American samples and European American samples. The $-\log_{10}(p)$ value of gene-SNP pairs adjusting for global ancestry (x-axis) is positively correlated with the $-\log_{10}(p)$ value of gene-SNP pairs adjusting for local ancestry (y-axis) in African Americans (A) and European Americans (B).

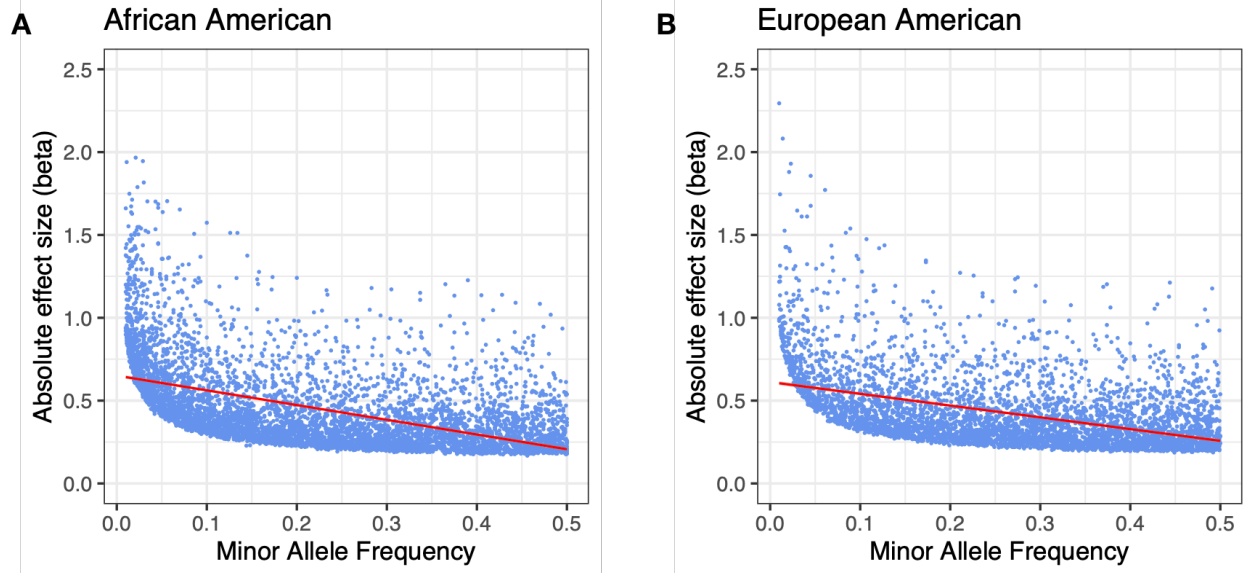


Figure S4. Negative correlation between eQTL minor allele frequency and its absolute effect size. The absolute value of the eQTL effect size (y-axis) is negatively correlated eQTL minor allele frequency (x-axis) in African Americans (A) and European Americans (B).

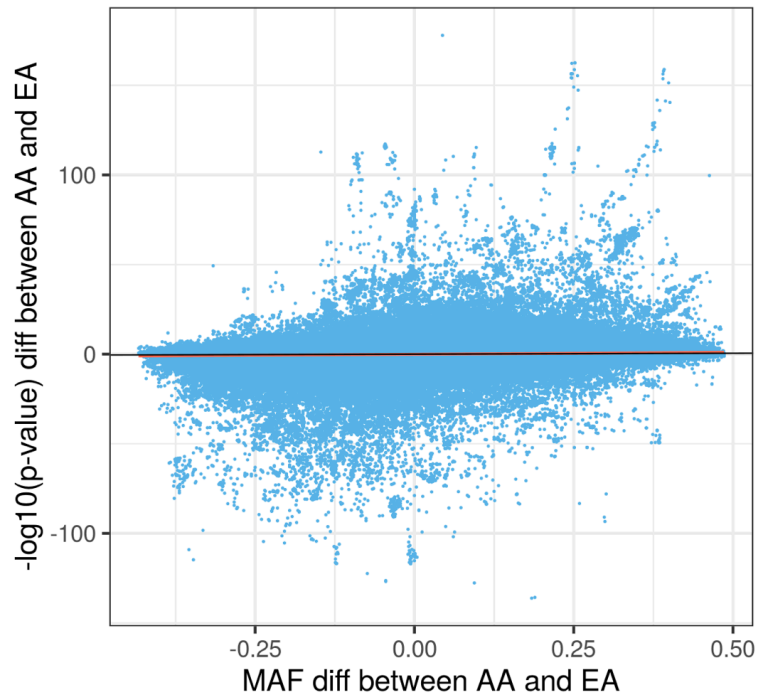


Figure S5. Relationship between the MAF difference and the $-\log_{10}(\text{pvalue})$ difference in African Americans and European Americans. The difference in $-\log_{10}(\text{p value})$ of gene-SNP pairs (y-axis) between African Americans and European Americans is positively correlated with the difference in MAF (x-axis) between the two populations.

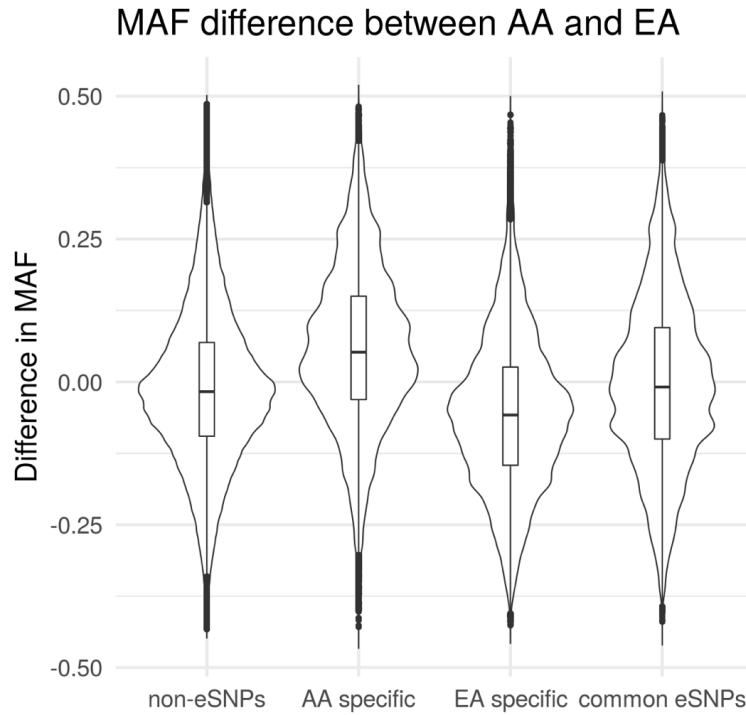


Figure S6. MAF difference between African Americans and European Americans for four eSNP categories. The four eSNP categories include non-eSNPs, AA specific eSNPs, EA specific eSNPs, and common eSNPs. The AA specific eSNPs tend to have higher MAF in AA than in EA while the EA specific eSNPs tend to have higher MAF in EA than in AA.

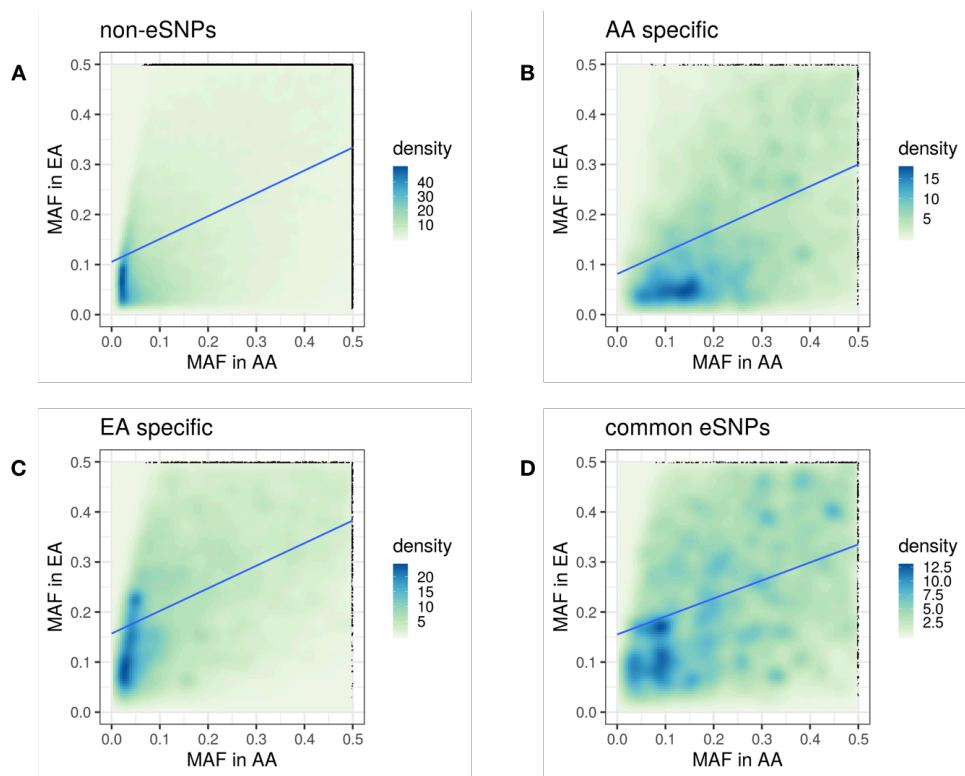


Figure S7. MAF density plot in four SNP categories in African Americans and European Americans. The four eSNP categories include non-eSNPs (A), AA specific eSNPs (B), EA specific eSNPs (C), and common eSNPs (D). The AA specific eSNPs tend to have higher MAF in AA than in EA while the EA specific eSNPs tend to have higher MAF in EA than in AA.

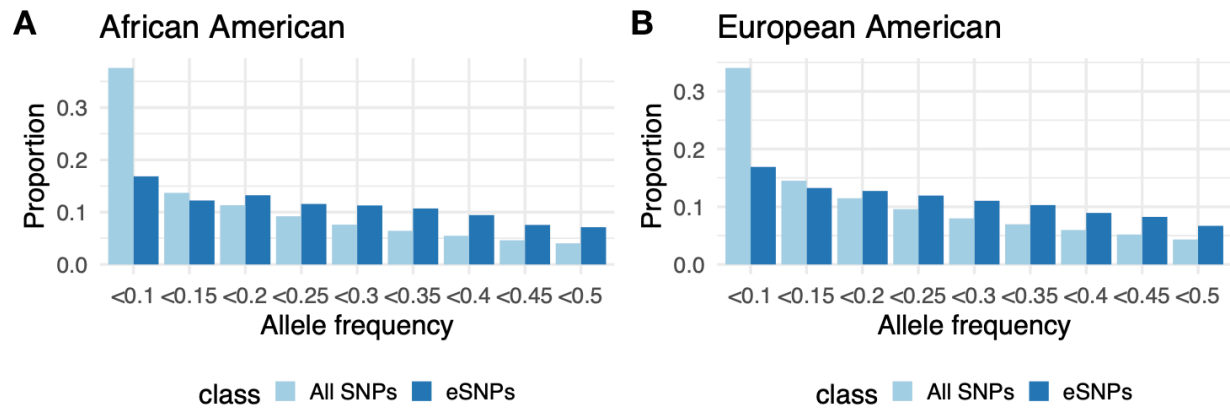


Figure S8. MAF distribution of all SNPs and eSNPs in African Americans and European Americans. The eSNPs tend to have higher MAF than tested SNPs in African American (A) and European American (B).

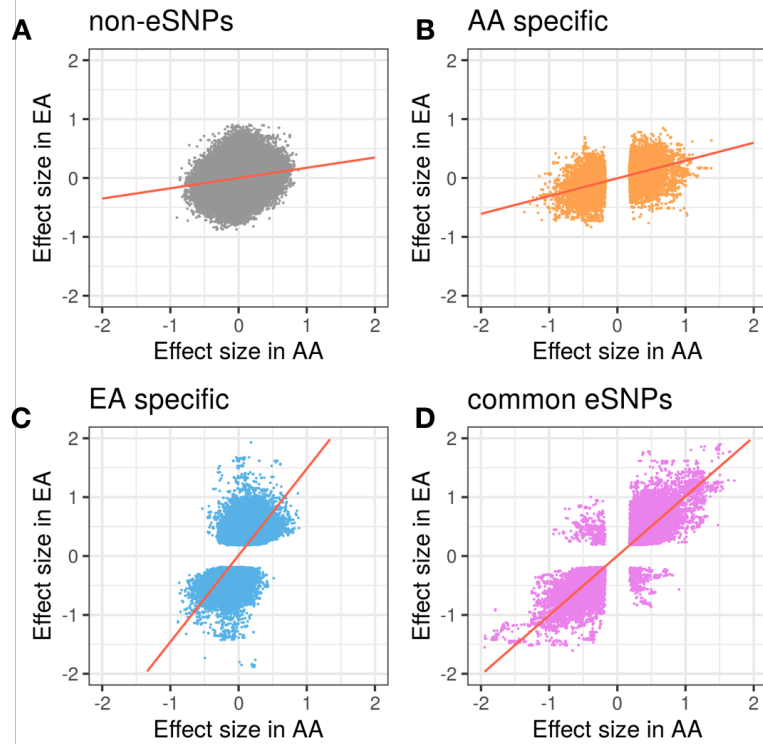


Figure S9. Effect sizes distribution of four categories of SNPs in African Americans and European Americans. The four eSNP categories include non-eSNPs (A), AA specific eSNPs (B), EA specific eSNPs (C), and common eSNPs (D). The EA unique eSNPs tends to have larger effect size in EA as compared to AA; and vice versa.

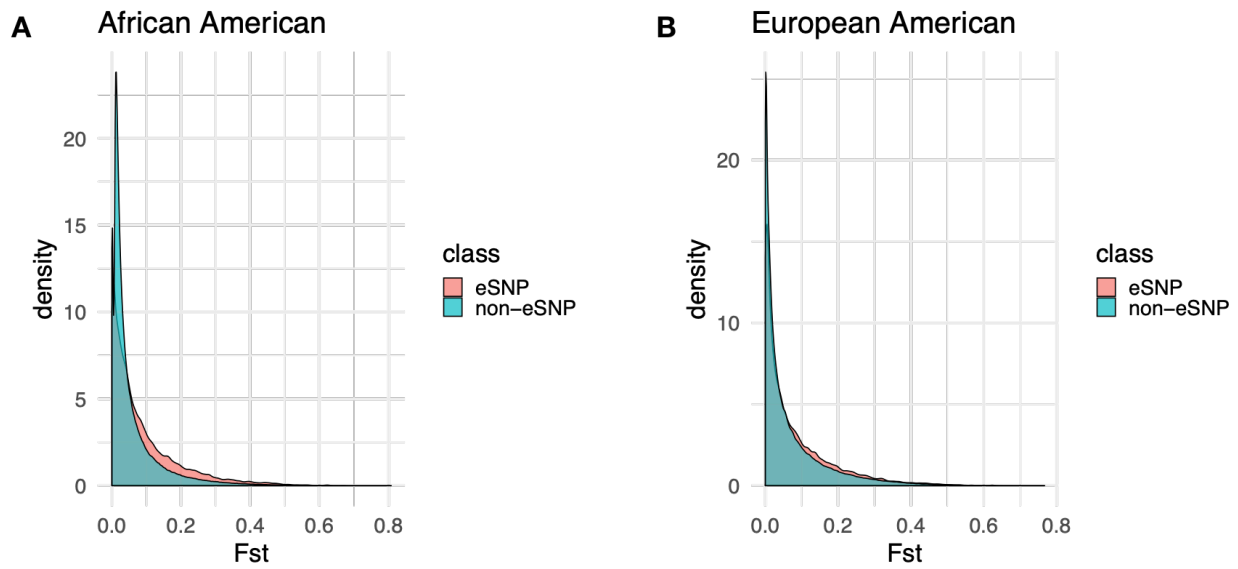


Figure S10. Density plot for F_{st} of eSNPs versus non-eSNPs. eSNPs tend to have larger F_{st} than non-eSNPs in both African Americans (A) and European Americans (B).

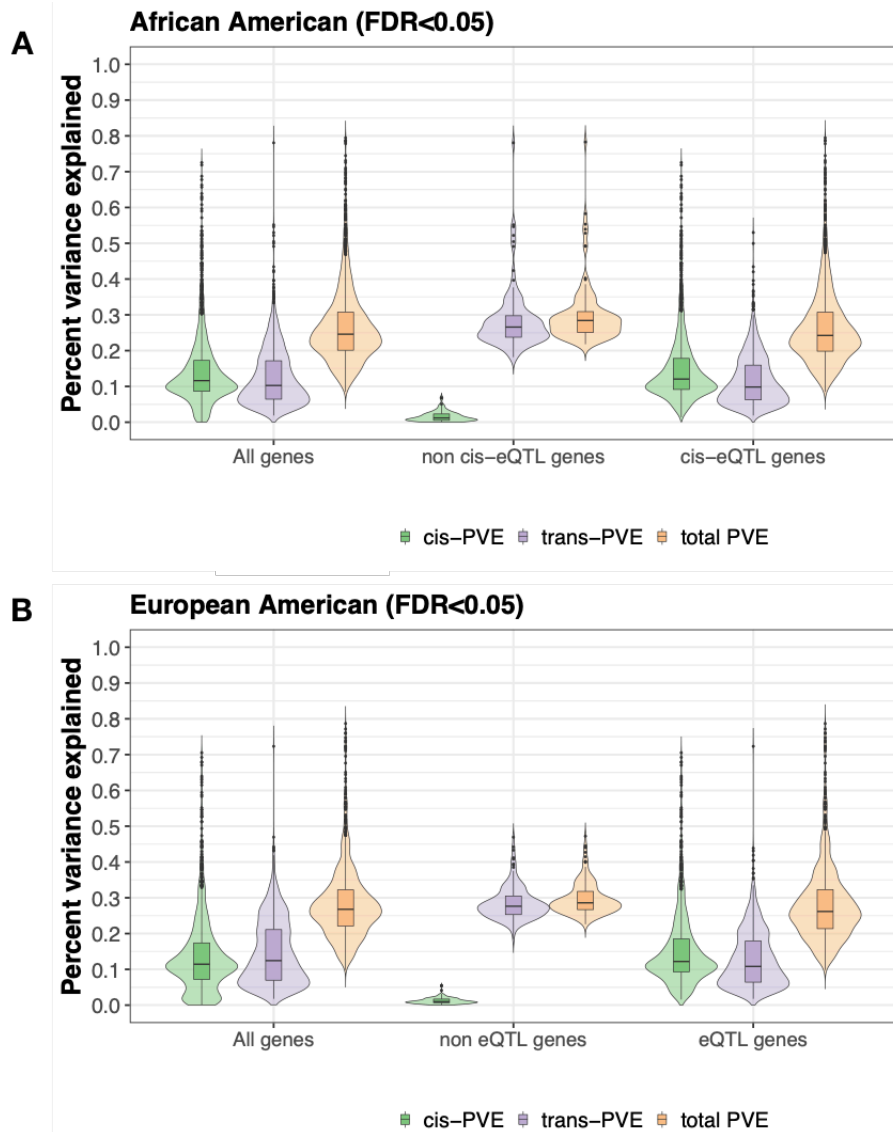


Figure S11. Estimation and partitioning of SNP heritability underlying gene expression variation in African Americans and European Americans. Proportion of variance (PVE; a.k.a. SNP heritability) in gene expression levels estimated for genes that have a PVE that significantly deviates from zero at $FDR < 0.05$: all genes (left three plots), genes without detectable eQTLs (middle three plots), and genes with detectable eQTLs (right three plots) in African Americans (**A**) and European Americans (**B**). PVE explained by all SNPs is referred to as total PVE (orange), which is partitioned into a component that is explained by cis-SNPs (cis-PVE; green) and another component that is explained by trans-SNPs (trans-PVE; purple). As expected, PVE in eGenes tends to be larger than that in non-eGenes or in all genes. The total PVE as well as the cis-PVE in cis-eQTL genes also tend to be larger than that in non cis-eQTL genes or in all genes.

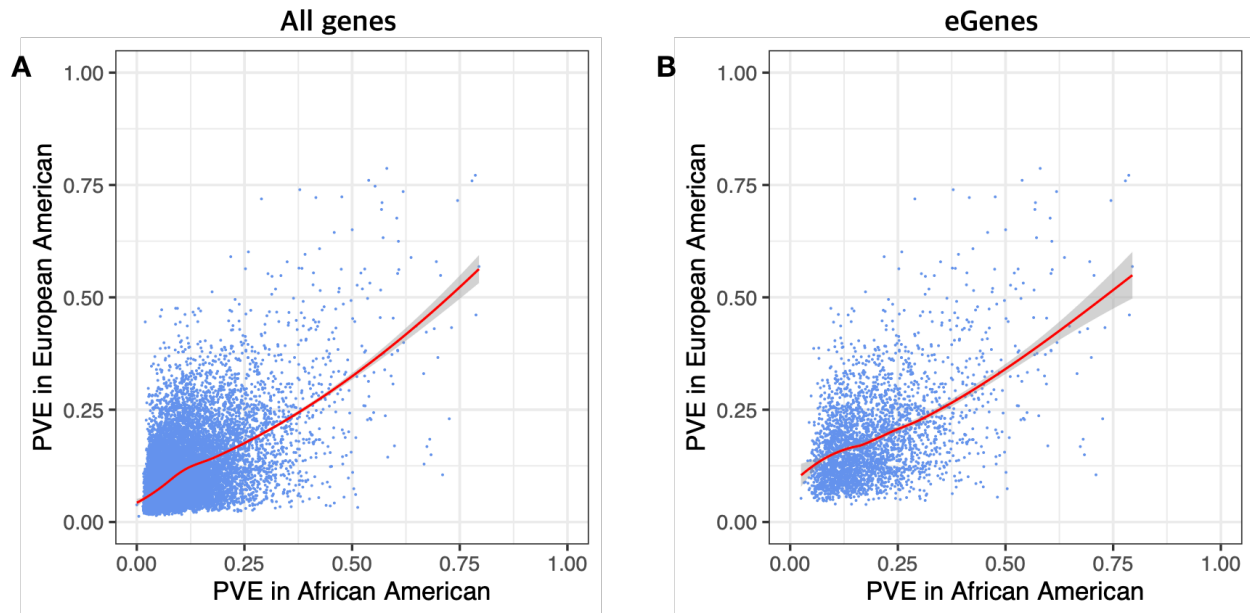


Figure S12. Comparison of SNP heritability of gene expression between African Americans and European Americans. The estimated SNP heritability (a.k.a. proportion of gene expression variance explained by all SNPs, or PVE) in European Americans (y-axis) is plotted against that in African Americans (x-axis). Results are shown for all genes (A) or eGenes (B). On both plots, each dot represents a gene and the blue curve is the fitted loess smooth line. Estimated SNP heritability of gene expression is consistent between African Americans and European Americans.

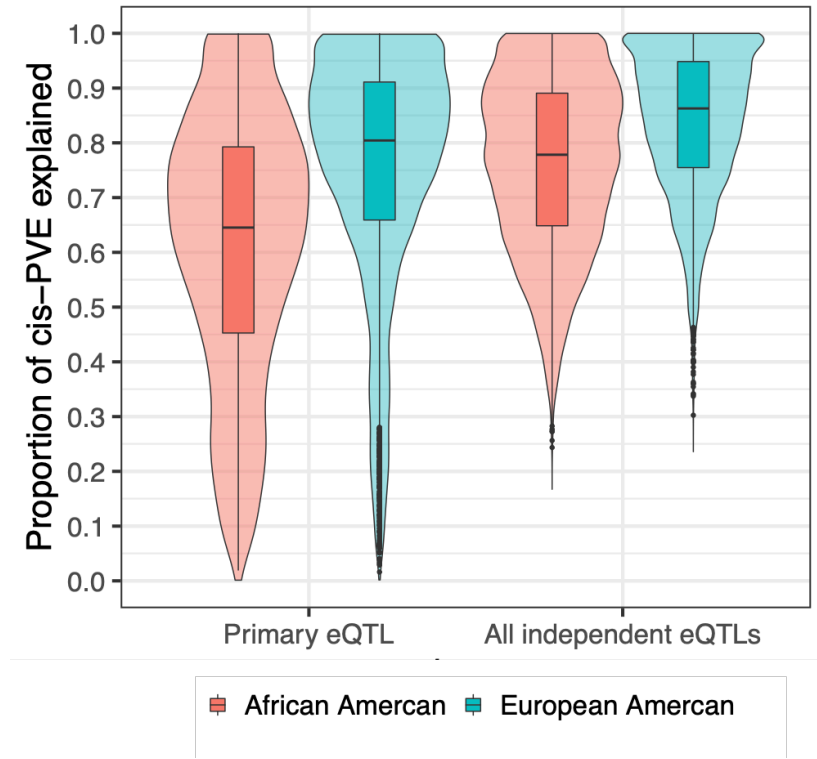
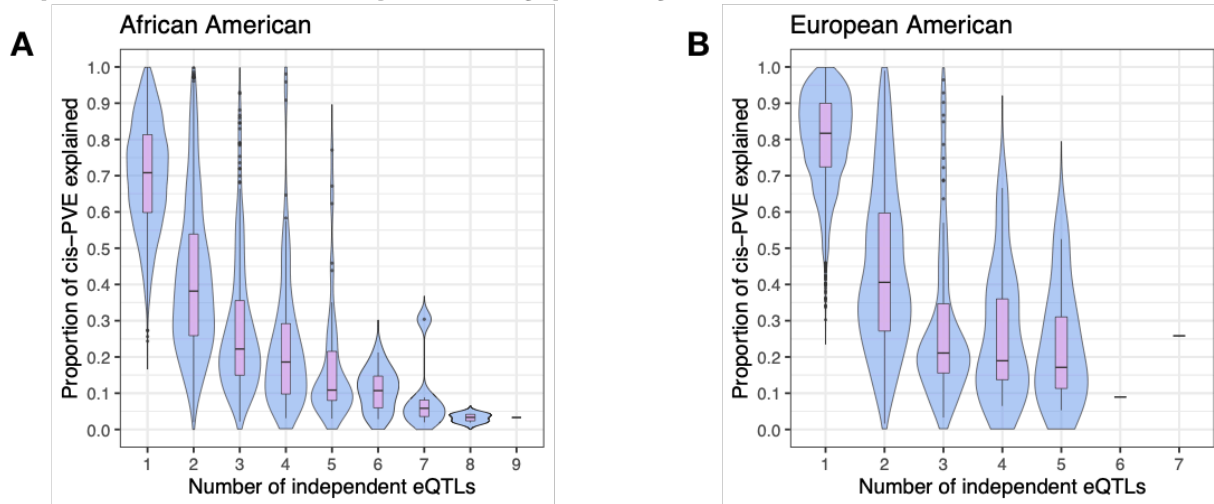


Figure S13. Violin Plot shows the proportion of cis-SNP heritability explained by identified independent eQTLs in eGenes. Results are obtained through BSLMM and are shown for African Americans and European Americans. The identified primary and all independent eQTLs generally explains a large proportion of cis-SNP heritability.

Proportion of cis-PVE explained by primary eQTLs



Proportion of cis-PVE explained by independent eQTLs

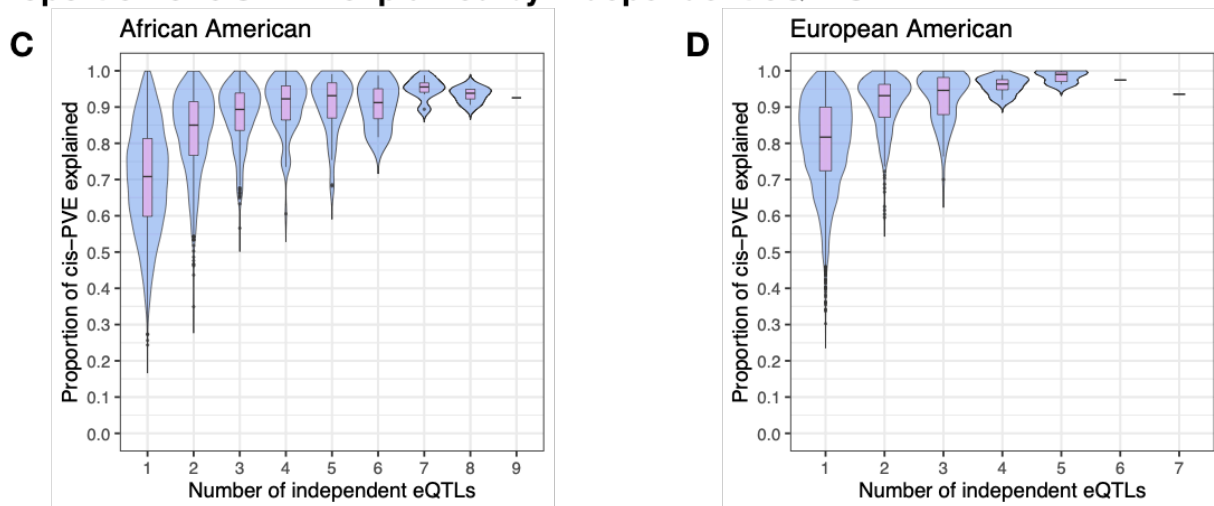


Figure S14. The proportion of cis-SNP heritability for gene expression explained by identified primary eQTLs and independent eQTLs depends on the number of eQTLs identified. Violin plots show the proportion of cis-SNP heritability explained by identified primary eQTLs (y-axis) (A, B) and all independent eQTLs (C,D) with respect to the number of identified independent eQTLs (x-axis) in eGenes. Results are shown for African Americans (A,C) and European Americans (B,D).

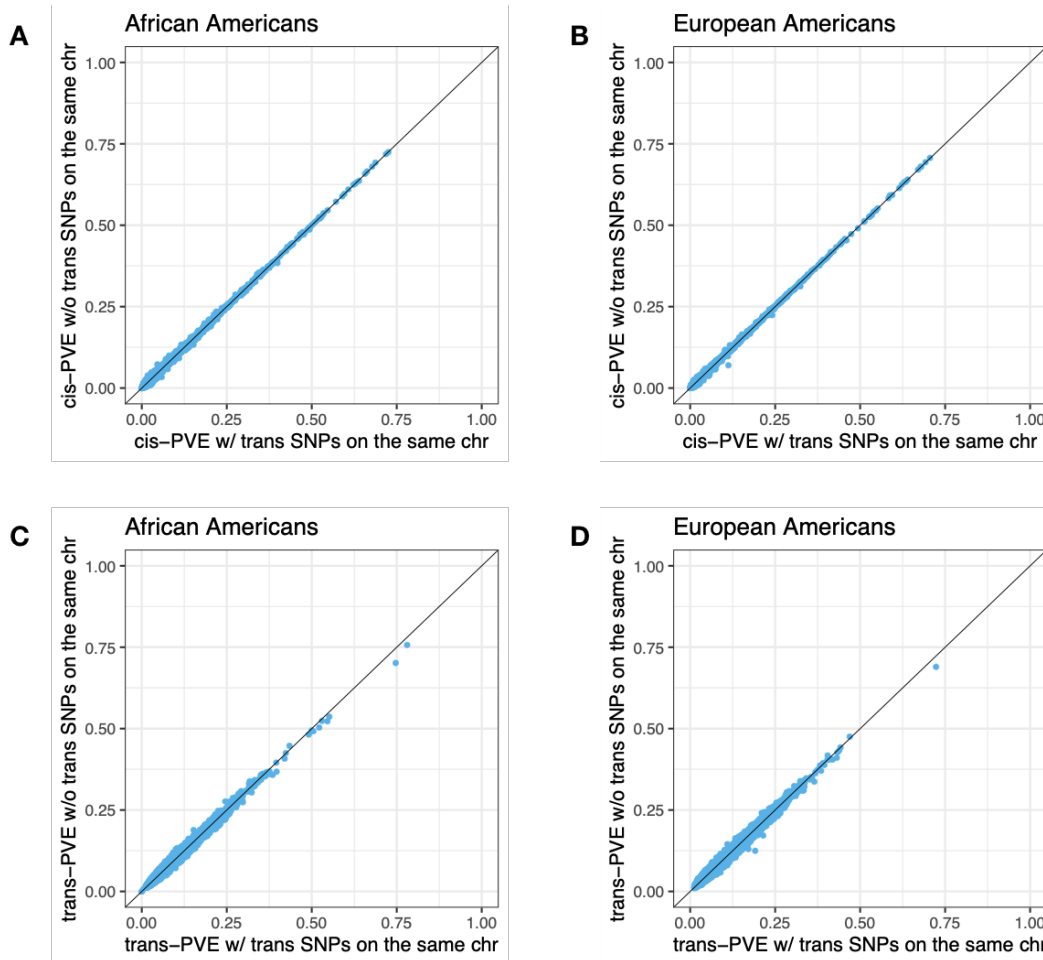


Figure S15. cis-PVE and trans-PVE comparison for two analytic approaches in African American and European American. The first analytic approach (x-axis) uses trans SNPs on the same chromosome while the second analytic approach (y-axis) does not use trans SNPs on the same chromosome. The cis heritability (cis-PVE) estimates obtained using trans SNPs residing on the other chromosomes are almost identical to the estimates obtained using SNPs on all chromosomes in both African American (A) and European American (B). The trans heritability (trans-PVE) estimates obtained using trans SNPs residing on the other chromosomes are also almost identical to the estimates obtained using SNPs on all chromosomes in both African American (C) and European American (D).

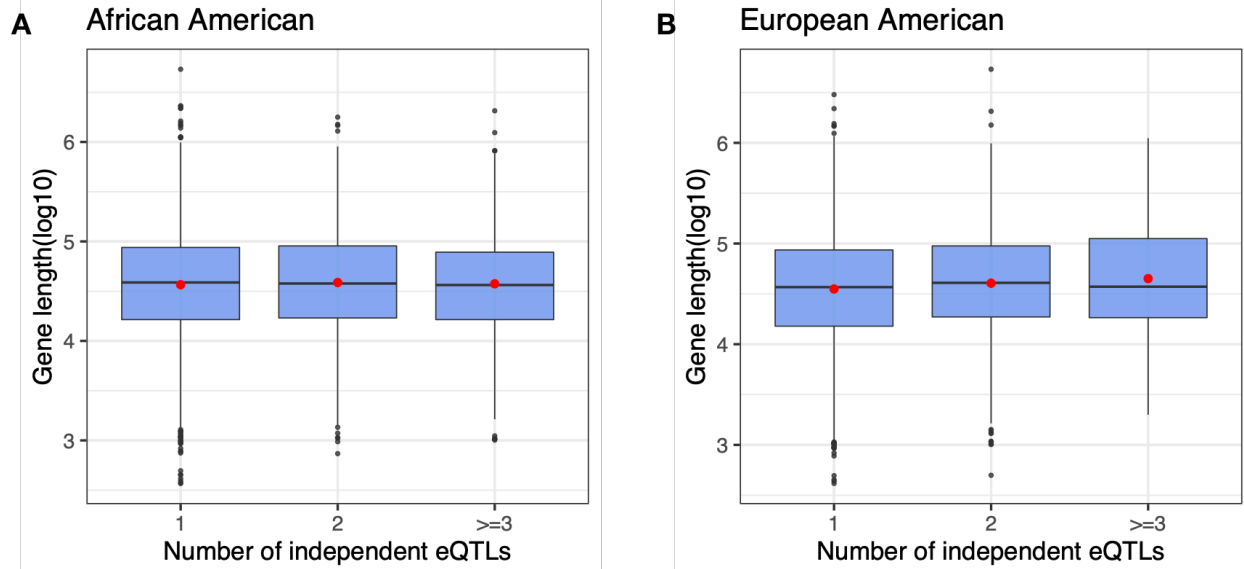


Figure S16. The number of independent eQTLs identified in eGenes depends on the gene length. Boxplot of log10 transformed gene length (y-axis) is shown across three eGene groups: eGenes that contain only the primary eQTL, eGenes that contain two independent eQTLs, and eGenes that contain more than three independent eQTLs. Results are shown for African Americans (A) and European Americans (B). Red dot on the plots represent the mean. eGenes with a larger number of independent eQTLs tend to have larger gene length.

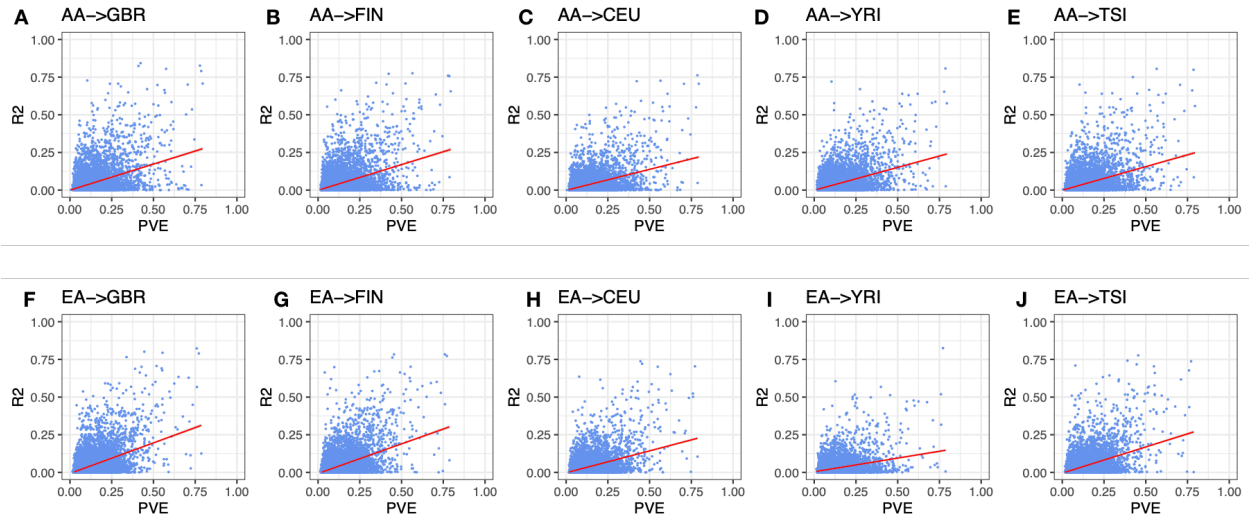


Figure S17. Accuracy of gene expression prediction depends on the SNP heritability of gene expression. Scatter plots show the prediction performance measured by R^2 (y-axis) versus the SNP heritability of gene expression (x-axis). Each dot represents a gene. Title of each plot shows the population in GENOA used for constructing the gene expression prediction model and the population in Geuvadis used for measuring prediction performance. For example, AA -> GBR represents that the gene expression prediction model is constructed in the GENOA AA population while its performance is measured in the Geuvadis GBR population. The GENOA population used for constructing the gene expression prediction model include African Americans (**A-E**) and European Americans (**F-J**).

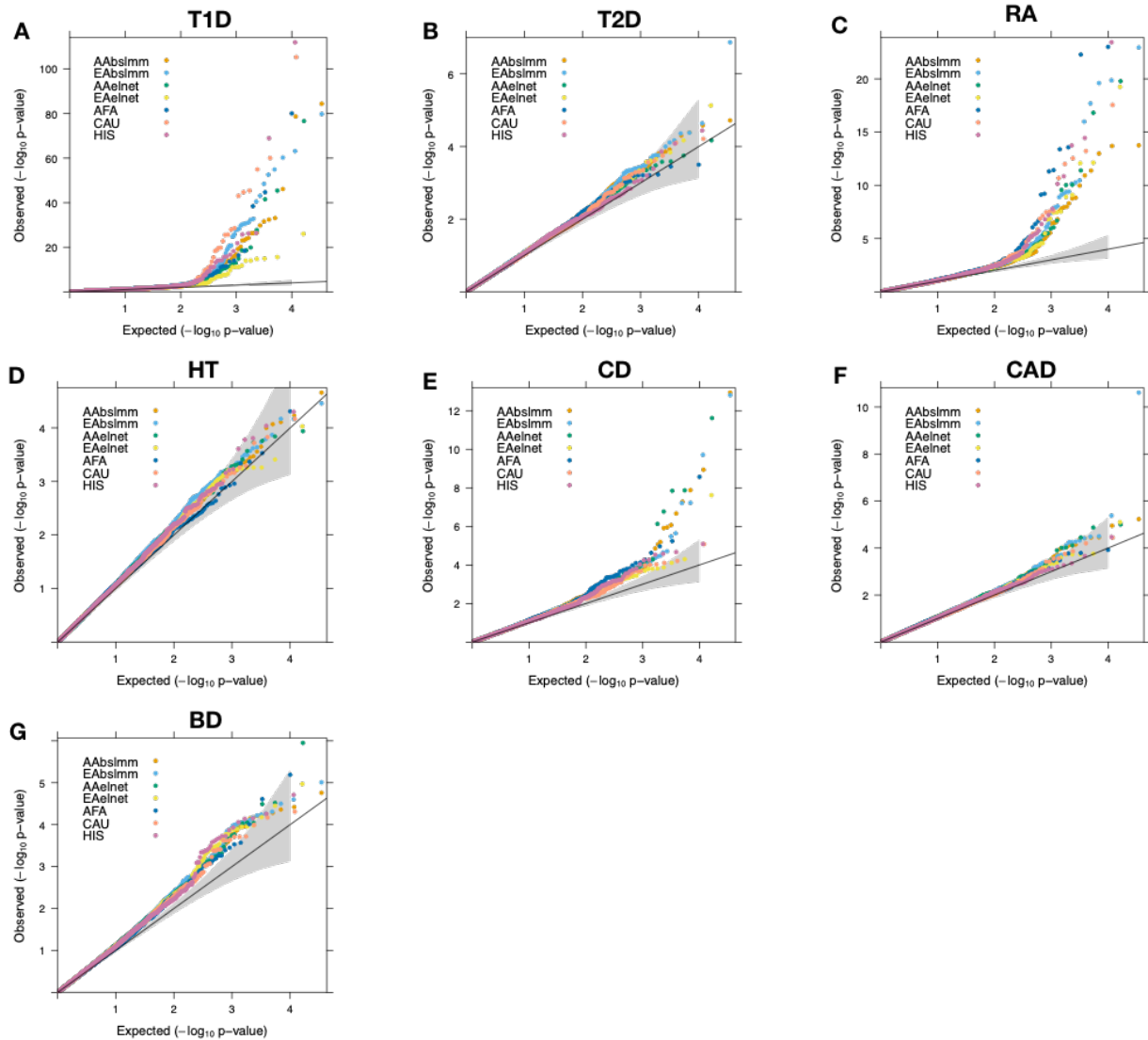


Figure S18. Transcriptome wide association study for seven diseases in WTCCC. Q-Q plots display the $-\log_{10} p$ -values (y-axis) from TWAS analysis using gene expression models constructed based on different populations versus the expected null (x-axis). The five populations used to construct the gene expression models include GENOA AA (yellow), GENOA EA (purple), MESA AFA (green), MESA HIS (pink), and MESA CAU (blue). Results are shown for each of the seven diseases in WTCCC that include Crohn’s disease (CD), rheumatoid arthritis (RA), bipolar disorder (BD), type 1 diabetes (T1D), type 2 diabetes (T2D), coronary artery disease (CAD), and hypertension (HT) (A-G). In each panel, the shaded grey line/area represent the point-wise 95% confidence interval.

Table S1. Comparison of eQTL mapping results for African Americans and European Americans in GENOA. The first row shows the number of eGenes that are identified in AA (first column), the total number of genes analyzed in AA (second column), the percentage of genes that are eGenes in AA (third column), the number of eGenes that are identified in EA (fourth column), the total number of genes analyzed in EA (fifth column), the percentage of genes that are eGenes in EA (sixth column), the number of common eGenes identified in both AA and EA (seventh column), the proportion of eGenes identified in AA that are also identified in EA (eighth column) and the proportion of eGenes identified in EA that are also identified in AA (ninth column).

FDR = 0.01

	African American (AA)			European American (EA)			Overlapping		
	Number	Total	Percentage	Number	Total	Percentage	Number	AA%	EA%
eGenes	4,433	17,572	25.23%	3,517	17,343	20.28%	2,350	53.01%	66.81%
eSNPs	278,473	14,511,338	1.92%	294,878	8,521,801	3.46%	88,971	31.95%	30.17%

FDR = 0.05

	African American (AA)			European American (EA)			Overlapping		
	Number	Total	Percentage	Number	Total	Percentage	Number	AA%	EA%
eGenes	5,475	17,572	31.16%	4,402	17,343	25.38%	3,048	55.67%	69.24%
eSNPs	354,931	14,511,338	2.45%	371,309	8,521,801	4.36%	112,316	31.64%	30.25%

FDR = 0.1

	African American (AA)			European American (EA)			Overlapping		
	Number	Total	Percentage	Number	Total	Percentage	Number	AA%	EA%
eGenes	6,172	17,572	35.12%	5,121	17,343	29.53%	3,540	57.36%	69.13%
eSNPs	404,971	14,511,338	2.79%	421,583	8,521,801	4.95%	126,564	31.25%	30.02%

FDR = 0.2

	African American (AA)			European American (EA)			Overlapping		
	Number	Total	Percentage	Number	Total	Percentage	Number	AA%	EA%
eGenes	7,256	17,572	41.29%	6,216	17,343	35.84%	4,292	59.15%	69.05%
eSNPs	473,459	14,511,338	3.26%	494,518	8,521,801	5.8%	146,684	30.98%	29.66%

Table S2. Comparison of eQTL mapping results for African Americans and European Americans. True positive rate π_1 statistics for cis-eQTLs are listed comparing each discovery population (two rows) to each replication population (7 columns). Higher π_1 values indicate a stronger replication signal. π_1 is calculated on SNP-gene pairs that are available both in the discovery population and the replication population.

	GENOA AA (n=1,205)	GENOA EA (n=801)	MESA AFA (n=233)	MESA CAU (n=578)	MESA HIS (n=352)	Geuvadis YRI (n=89)	Geuvadis EUR (n=373)
GENOA AA	1	0.834	0.593	0.69	0.633	0.693	0.919
GENOA EA	0.752	1	0.514	0.727	0.705	0.699	0.909

Table S3. Comparison of eQTL mapping results for African Americans and European Americans in the GENOA study adjusting for local ancestry and global ancestry. The first row shows the number of eGenes that are identified in AA adjusting for local ancestry (LA) (first column), the number of eGenes that are identified in AA adjusting for global ancestry (GA) (second column), the number of genes that are overlapped eGenes in LA and GA in AA (third column), the number of eGenes that are identified in EA adjusting for local ancestry (fourth column), the number of eGenes that are identified in EA adjusting for global ancestry (fifth column), the number of genes that are overlapped eGenes in LA and GA in EA (sixth column).

	African American			European American		
	Local Ancestry	Global Ancestry	Overlap	Local Ancestry	Global Ancestry	Overlap
eGenes	5,553	5,475	5,312	4,586	4,402	4,333
eSNPs	357,072	354,931	325,571	372,240	371,309	347,949

Table S4. Gene Ontology analysis identifies molecular functions that are enriched in eGenes in African American in GENOA. Table lists the data source, GO terms, GO term id, and adjusted enrichment p-values.

Source	Term name	Term id	Adjusted p value
GO:MF	catalytic activity	GO:0003824	8.45E-37
GO:MF	binding	GO:0005488	2.81E-18
GO:MF	Molecular function	GO:0003674	1.45E-16
GO:MF	transferase activity	GO:0016740	4.07E-12
GO:MF	protein binding	GO:0005515	5.26E-07
GO:MF	ion binding	GO:0043167	1.0347E-06
GO:MF	nucleoside phosphate binding	GO:1901265	3.578E-06
GO:MF	nucleotide binding	GO:0000166	3.578E-06
GO:MF	oxidoreductase activity	GO:0016491	4.8963E-06
GO:MF	coenzyme binding	GO:0050662	7.9074E-06
GO:MF	heterocyclic compound binding	GO:1901363	8.2704E-06

Table S5. Gene Ontology analysis identifies biological processes that are enriched in eGenes in African American in GENOA. Table lists the data source, GO terms, GO term id, and adjusted enrichment p-values.

Source	Term name	Term id	Adjusted p value
GO:BP	cellular metabolic process	GO:0044237	1.92E-31
GO:BP	metabolic process	GO:0008152	6.32E-31
GO:BP	organic substance metabolic process	GO:0071704	1.33E-21
GO:BP	primary metabolic process	GO:0044238	1.34E-17
GO:BP	nitrogen compound metabolic process	GO:0006807	3.48E-16
GO:BP	organonitrogen compound biosynthetic process	GO:1901566	4.70E-13
GO:BP	small molecule metabolic process	GO:0044281	1.49E-12
GO:BP	cellular nitrogen compound metabolic process	GO:0034641	2.89E-11
GO:BP	cellular catabolic process	GO:0044248	2.90E-11
GO:BP	organonitrogen compound metabolic process	GO:1901564	7.61E-10
GO:BP	establishment of protein localization	GO:0045184	4.22E-09
GO:BP	oxidation-reduction process	GO:0055114	5.65E-09
GO:BP	cellular amide metabolic process	GO:0043603	1.35E-08
GO:BP	catabolic process	GO:0009056	3.36E-08
GO:BP	intracellular transport	GO:0046907	5.36E-08
GO:BP	Biological process	GO:0008150	5.49E-08
GO:BP	cofactor metabolic process	GO:0051186	6.46E-08
GO:BP	carboxylic acid metabolic process	GO:0019752	8.09E-08
GO:BP	ncRNA metabolic process	GO:0034660	1.26E-07
GO:BP	peptide transport	GO:0015833	1.27E-07
GO:BP	amide transport	GO:0042886	1.39E-07
GO:BP	protein transport	GO:0015031	1.45E-07
GO:BP	oxoacid metabolic process	GO:0043436	1.83E-07
GO:BP	ncRNA processing	GO:0034470	4.07E-07
GO:BP	protein localization	GO:0008104	4.29E-07
GO:BP	DNA repair	GO:0006281	4.68E-07
GO:BP	organic acid metabolic process	GO:0006082	6.30E-07
GO:BP	cellular process	GO:0009987	2.4288E-06
GO:BP	heterocycle metabolic process	GO:0046483	3.0713E-06
GO:BP	cellular localization	GO:0051641	3.5673E-06
GO:BP	organelle organization	GO:0006996	3.87E-06
GO:BP	organic cyclic compound metabolic process	GO:1901360	4.6015E-06
GO:BP	tRNA metabolic process	GO:0006399	5.0127E-06
GO:BP	macromolecule localization	GO:0033036	5.4124E-06

Table S6. Gene Ontology analysis identifies cellular components that are enriched in eGenes in GENOA. Table lists the data source, GO terms, GO term id, and adjusted enrichment p-values.

Source	Term name	Term id	Adjusted p value
GO:CC	intracellular	GO:0005622	4.69E-71
GO:CC	intracellular part	GO:0044424	1.90E-70
GO:CC	intracellular membrane-bounded organelle	GO:0043231	5.43E-58
GO:CC	intracellular organelle	GO:0043229	2.31E-54
GO:CC	cytoplasmic part	GO:0044444	4.17E-50
GO:CC	membrane-bounded organelle	GO:0043227	6.82E-50
GO:CC	organelle	GO:0043226	1.86E-49
GO:CC	cytoplasm	GO:0005737	3.19E-47
GO:CC	mitochondrion	GO:0005739	4.38E-37
GO:CC	cytosol	GO:0005829	2.27E-29
GO:CC	intracellular organelle part	GO:0044446	4.02E-29
GO:CC	cell part	GO:0044464	1.88E-26
GO:CC	cell	GO:0005623	3.48E-26
GO:CC	mitochondrial part	GO:0044429	5.14E-26
GO:CC	organelle part	GO:0044422	2.50E-25
GO:CC	mitochondrial matrix	GO:0005759	3.83E-19
GO:CC	nucleus	GO:0005634	1.61E-14
GO:CC	organelle membrane	GO:0031090	6.58E-13
GO:CC	mitochondrial envelope	GO:0005740	2.80E-11
GO:CC	envelope	GO:0031975	1.84E-10
GO:CC	organelle envelope	GO:0031967	1.84E-10
GO:CC	protein-containing complex	GO:0032991	2.99E-09
GO:CC	membrane-enclosed lumen	GO:0031974	4.68E-09
GO:CC	organelle lumen	GO:0043233	4.68E-09
GO:CC	intracellular organelle lumen	GO:0070013	4.68E-09
GO:CC	mitochondrial membrane	GO:0031966	5.83E-09
GO:CC	vacuole	GO:0005773	6.29E-08
GO:CC	nucleoplasm	GO:0005654	1.86E-07
GO:CC	Cellular component	GO:0005575	7.33E-07
GO:CC	lysosome	GO:0005764	2.5594E-06
GO:CC	lytic vacuole	GO:0000323	2.5594E-06

Table S7. Gene Ontology analysis identifies human phenotype that are enriched in eGenes in African American in GENOA. Table lists the data source, GO terms, GO term id, and adjusted enrichment p-values.

Source	Term name	Term id	Adjusted p value
HP	Abnormality of central motor function	HP:0011442	3.15E-14
HP	Upper motor neuron dysfunction	HP:0002493	9.65E-10
HP	Hypertonia	HP:0001276	1.80E-09
HP	Abnormal muscle tone	HP:0003808	2.65E-09
HP	Abnormality of the cerebrum	HP:0002060	4.92E-09
HP	Atrophy/Degeneration affecting the central nervous system	HP:0007367	7.22E-09
HP	Abnormality of the cerebral subcortex	HP:0010993	8.96E-09
HP	Abnormality of forebrain morphology	HP:0100547	9.86E-09
HP	Autosomal recessive inheritance	HP:0000007	1.30E-08
HP	Cerebral atrophy	HP:0002059	1.43E-08
HP	Atrophy/Degeneration affecting the cerebrum	HP:0007369	1.74E-08
HP	Brain atrophy	HP:0012444	2.74E-08
HP	Generalized hypotonia	HP:0001290	6.88E-08
HP	Abnormality of movement	HP:0100022	9.53E-08
HP	Aplasia/Hypoplasia involving the central nervous system	HP:0002977	1.92E-07
HP	Abnormality of coordination	HP:0011443	2.55E-07
HP	Spasticity	HP:0001257	2.78E-07

HP	Ataxia	HP:0001251	2.87E-07
HP	Muscular hypotonia	HP:0001252	3.67E-07
HP	Lactic acidosis	HP:0003128	6.07E-07
HP	Seizures	HP:0001250	7.96E-07
HP	Dystonia	HP:0001332	9.94E-07
HP	Abnormal muscle physiology	HP:0011804	3.0589E-06
HP	Abnormality of the musculature	HP:0003011	4.3264E-06
HP	Abnormality of the cerebral white matter	HP:0002500	4.6036E-06
HP	Aplasia/Hypoplasia of the cerebrum	HP:0007364	4.7496E-06
HP	Neurodevelopmental abnormality	HP:0012759	8.8099E-06

Table S8. Gene Ontology analysis identifies molecular functions that are enriched in eGenes in European American in GENOA. Table lists the data source, GO terms, GO term id, and adjusted enrichment p-values.

Source	Term name	Term id	Adjusted p value
GO:MF	catalytic activity	GO:0003824	4.12E-18
GO:MF	coenzyme binding	GO:0050662	7.5694E-06

Table S9. Gene Ontology analysis identifies biological processes that are enriched in eGenes in European American in GENOA. Table lists the data source, GO terms, GO term id, and adjusted enrichment p-values.

Source	Term name	Term id	Adjusted p value
GO:BP	small molecule metabolic process	GO:0044281	3.90E-10
GO:BP	metabolic process	GO:0008152	1.06E-09
GO:BP	cellular metabolic process	GO:0044237	1.27E-09
GO:BP	organophosphate metabolic process	GO:0019637	1.8622E-06
GO:BP	organonitrogen compound biosynthetic process	GO:1901566	6.5114E-06

Table S10. Gene Ontology analysis identifies cellular components that are enriched in eGenes in European American in GENOA. Table lists the data source, GO terms, GO term id, and adjusted enrichment p-values.

Source	Term name	Term id	Adjusted p value
GO:CC	intracellular	GO:0005622	1.01E-35
GO:CC	intracellular part	GO:0044424	3.39E-34
GO:CC	cytoplasmic part	GO:0044444	7.15E-25
GO:CC	membrane-bounded organelle	GO:0043227	7.00E-23
GO:CC	intracellular membrane-bounded organelle	GO:0043231	1.58E-22
GO:CC	cytoplasm	GO:0005737	4.77E-22
GO:CC	intracellular organelle	GO:0043229	1.22E-20
GO:CC	organelle	GO:0043226	1.10E-19
GO:CC	mitochondrion	GO:0005739	3.18E-17
GO:CC	mitochondrial part	GO:0044429	7.69E-14
GO:CC	cytosol	GO:0005829	1.43E-09
GO:CC	cell part	GO:0044464	2.03E-09
GO:CC	mitochondrial matrix	GO:0005759	5.66E-09
GO:CC	cell	GO:0005623	2.29E-08
GO:CC	intracellular organelle part	GO:0044446	4.87E-08
GO:CC	organelle part	GO:0044422	1.3891E-06
GO:CC	organelle membrane	GO:0031090	8.736E-06

Table S11. Gene Ontology analysis identifies human phenotype that are enriched in eGenes in European American in GENOA. Table lists the data source, GO terms, GO term id, and adjusted enrichment p-values.

Source	Term name	Term id	Adjusted p value
HP	Autosomal recessive inheritance	HP:0000007	5.1487E-06

Table S12. Gene Ontology analysis in molecular functions for genes without eQTL in African American in GENOA. Table lists the data source, GO terms, GO term id, and adjusted enrichment p-values.

Source	Term name	Term id	Adjusted p value
GO:MF	G protein-coupled receptor activity	GO:0004930	2.80E-25
GO:MF	transmembrane signaling receptor activity	GO:0004888	4.96E-21
GO:MF	signaling receptor activity	GO:0038023	4.56E-19
GO:MF	molecular transducer activity	GO:0060089	4.61E-18
GO:MF	olfactory receptor activity	GO:0004984	2.40E-17
GO:MF	transcription regulatory region sequence-specific DNA binding	GO:0000976	4.44E-14
GO:MF	RNA polymerase II regulatory region DNA binding	GO:0001012	3.83E-13
GO:MF	RNA polymerase II regulatory region sequence-specific DNA binding	GO:0000977	5.47E-13
GO:MF	sequence-specific double-stranded DNA binding	GO:1990837	1.07E-12
GO:MF	receptor regulator activity	GO:0030545	4.27E-12
GO:MF	DNA-binding transcription factor activity, RNA polymerase II-specific	GO:0000981	5.38E-12
GO:MF	transcription regulatory region DNA binding	GO:0044212	8.80E-12
GO:MF	regulatory region nucleic acid binding	GO:0001067	1.46E-11
GO:MF	receptor ligand activity	GO:0048018	1.54E-11
GO:MF	signaling receptor activator activity	GO:0030546	1.01E-10
GO:MF	sequence-specific DNA binding	GO:0043565	4.06E-10
GO:MF	double-stranded DNA binding	GO:0003690	2.35E-08
GO:MF	signaling receptor binding	GO:0005102	2.81E-08
GO:MF	proximal promoter sequence-specific DNA binding	GO:0000987	3.23E-07
GO:MF	RNA polymerase II proximal promoter sequence-specific DNA binding	GO:0000978	2.7732E-06
GO:MF	DNA-binding transcription activator activity	GO:0001216	5.2714E-06
GO:MF	DNA-binding transcription activator activity, RNA polymerase II-specific	GO:0001228	6.3852E-06

Table S13. Gene Ontology analysis in biological processes for genes without eQTL in African American in GENOA. Table lists the data source, GO terms, GO term id, and adjusted enrichment p-values.

Source	Term name	Term id	Adjusted p value
GO:BP	multicellular organismal process	GO:0032501	4.85E-26
GO:BP	G protein-coupled receptor signaling pathway	GO:0007186	2.61E-23
GO:BP	detection of stimulus involved in sensory perception	GO:0050906	8.46E-20
GO:BP	sensory perception	GO:0007600	2.60E-19
GO:BP	detection of chemical stimulus involved in sensory perception	GO:0050907	3.40E-19
GO:BP	system process	GO:0003008	2.16E-18
GO:BP	nervous system process	GO:0050877	2.64E-18
GO:BP	sensory perception of chemical stimulus	GO:0007606	2.37E-17
GO:BP	detection of chemical stimulus involved in sensory perception of smell	GO:0050911	2.40E-17
GO:BP	detection of chemical stimulus	GO:0009593	6.74E-17
GO:BP	sensory perception of smell	GO:0007608	6.33E-16
GO:BP	multicellular organism development	GO:0007275	8.43E-16
GO:BP	detection of stimulus	GO:0051606	4.11E-15
GO:BP	system development	GO:0048731	2.29E-14
GO:BP	anatomical structure development	GO:0048856	3.01E-13
GO:BP	developmental process	GO:0032502	4.94E-13
GO:BP	animal organ development	GO:0048513	1.01E-12
GO:BP	keratinization	GO:0031424	1.54E-11
GO:BP	cell differentiation	GO:0030154	7.81E-11

GO:BP	tissue development	GO:0009888	2.55E-10
GO:BP	cellular developmental process	GO:0048869	1.13E-09
GO:BP	epidermis development	GO:0008544	3.56E-09
GO:BP	signaling	GO:0023052	4.35E-09
GO:BP	cell communication	GO:0007154	9.41E-09
GO:BP	skin development	GO:0043588	9.63E-08
GO:BP	regulation of transcription by RNA polymerase II	GO:0006357	1.31E-07
GO:BP	cell fate commitment	GO:0045165	1.39E-07
GO:BP	signal transduction	GO:0007165	3.38E-07
GO:BP	epidermal cell differentiation	GO:0009913	4.30E-07
GO:BP	epithelial cell differentiation	GO:0030855	7.56E-07
GO:BP	nervous system development	GO:0007399	8.8929E-06

Table S14. Gene Ontology analysis in cellular components for genes without eQTL in African American in GENOA. Table lists the data source, GO terms, GO term id, and adjusted enrichment p-values.

Source	Term name	Term id	Adjusted p value
GO:CC	nuclear chromatin	GO:0000790	4.63E-14
GO:CC	cell periphery	GO:0071944	1.14E-11
GO:CC	plasma membrane	GO:0005886	1.20E-11
GO:CC	chromatin	GO:0000785	1.00E-10
GO:CC	intrinsic component of plasma membrane	GO:0031226	4.22E-10
GO:CC	extracellular matrix	GO:0031012	5.53E-10
GO:CC	integral component of plasma membrane	GO:0005887	1.72E-09
GO:CC	nuclear chromosome part	GO:0044454	1.89E-08
GO:CC	nuclear chromosome	GO:0000228	2.06E-07
GO:CC	plasma membrane part	GO:0044459	6.65E-07
GO:CC	intermediate filament	GO:0005882	7.03E-07
GO:CC	keratin filament	GO:0045095	3.2761E-06

Table S15. Gene Ontology analysis in human phenotype for genes without eQTL in African American in GENOA. Table lists the data source, GO terms, GO term id, and adjusted enrichment p-values.

Source	Term name	Term id	Adjusted p value
HP	Autosomal dominant inheritance	HP:0000006	5.2689E-06

Table S16. Gene Ontology analysis in molecular functions for genes without eQTL in European American in GENOA. Table lists the data source, GO terms, GO term id, and adjusted enrichment p-values.

Source	Term name	Term id	Adjusted p value
GO:MF	G protein-coupled receptor activity	GO:0004930	2.58E-12
GO:MF	olfactory receptor activity	GO:0004984	1.49E-09
GO:MF	molecular transducer activity	GO:0060089	1.83E-09
GO:MF	signaling receptor activity	GO:0038023	3.36E-09
GO:MF	DNA-binding transcription factor activity, RNA polymerase II-specific	GO:0000981	9.52E-09
GO:MF	sequence-specific double-stranded DNA binding	GO:1990837	1.25E-08
GO:MF	transcription regulatory region sequence-specific DNA binding	GO:0000976	1.39E-08
GO:MF	RNA polymerase II regulatory region sequence-specific DNA binding	GO:0000977	3.39E-08
GO:MF	transmembrane signaling receptor activity	GO:0004888	3.91E-08
GO:MF	RNA polymerase II regulatory region DNA binding	GO:0001012	5.74E-08
GO:MF	sequence-specific DNA binding	GO:0043565	1.06E-07
GO:MF	receptor regulator activity	GO:0030545	1.98E-07
GO:MF	double-stranded DNA binding	GO:0003690	2.4079E-06
GO:MF	receptor ligand activity	GO:0048018	3.7407E-06
GO:MF	signaling receptor activator activity	GO:0030546	3.836E-06

Table S17. Gene Ontology analysis in biological processes for genes without eQTL in European American in GENOA. Table lists the data source, GO terms, GO term id, and adjusted enrichment p-values.

Source	Term name	Term id	Adjusted p value
GO:BP	multicellular organismal process	GO:0032501	5.81E-21
GO:BP	system process	GO:0003008	1.09E-14
GO:BP	sensory perception	GO:0007600	1.65E-14
GO:BP	nervous system process	GO:0050877	1.77E-12
GO:BP	sensory perception of chemical stimulus	GO:0007606	6.28E-12
GO:BP	detection of stimulus involved in sensory perception	GO:0050906	9.49E-12
GO:BP	detection of chemical stimulus	GO:0009593	1.20E-11
GO:BP	detection of chemical stimulus involved in sensory perception	GO:0050907	2.07E-11
GO:BP	developmental process	GO:0032502	3.85E-11
GO:BP	detection of chemical stimulus involved in sensory perception of smell	GO:0050911	1.56E-09
GO:BP	multicellular organism development	GO:0007275	3.66E-09
GO:BP	sensory perception of smell	GO:0007608	3.68E-09
GO:BP	G protein-coupled receptor signaling pathway	GO:0007186	4.24E-09
GO:BP	system development	GO:0048731	5.14E-09
GO:BP	anatomical structure development	GO:0048856	7.00E-09
GO:BP	keratinization	GO:0031424	9.69E-09
GO:BP	cellular developmental process	GO:0048869	1.08E-08
GO:BP	cell differentiation	GO:0030154	1.10E-08
GO:BP	animal organ development	GO:0048513	3.65E-08
GO:BP	regulation of transcription by RNA polymerase II	GO:0006357	6.66E-08
GO:BP	detection of stimulus	GO:0051606	1.04E-07
GO:BP	epidermis development	GO:0008544	1.06E-07
GO:BP	signaling	GO:0023052	2.06E-07
GO:BP	cell communication	GO:0007154	2.83E-07
GO:BP	tissue development	GO:0009888	2.85E-07
GO:BP	epithelial cell differentiation	GO:0030855	3.84E-07
GO:BP	transcription by RNA polymerase II	GO:0006366	4.13E-07
GO:BP	epithelium development	GO:0060429	8.06E-07
GO:BP	epidermal cell differentiation	GO:0009913	1.6386E-06
GO:BP	keratinocyte differentiation	GO:0030216	1.7307E-06
GO:BP	skin development	GO:0043588	2.7064E-06
GO:BP	signal transduction	GO:0007165	4.3898E-06

Table S18. Gene Ontology analysis in cellular components for genes without eQTL in European American in GENOA. Table lists the data source, GO terms, GO term id, and adjusted enrichment p-values.

Source	Term name	Term id	Adjusted p value
GO:CC	nuclear chromatin	GO:0000790	2.46E-10
GO:CC	chromatin	GO:0000785	1.90E-09
GO:CC	nuclear chromosome part	GO:0044454	6.71E-07
GO:CC	nuclear chromosome	GO:0000228	2.1248E-06
GO:CC	intrinsic component of plasma membrane	GO:0031226	4.9426E-06

Table S19. Gene Ontology analysis in human phenotype for genes without eQTL in European American in GENOA. Table lists the data source, GO terms, GO term id, and adjusted enrichment p-values.

Source	Term name	Term id	Adjusted p value
HP	Autosomal dominant inheritance	HP:0000006	2.24E-11

Table S20. Gene Ontology and KEGG analysis in GOfuncR for genes with eQTL in African American in GENOA. Table lists the data source, GO term id, GO terms, and family wise error rate (FWER).

Ontology	Node id	Node name	FWER
Cellular component	GO:0005622	intracellular	0
Cellular component	GO:0043231	intracellular membrane-bounded organelle	0
Cellular component	GO:0043229	intracellular organelle	0
Cellular component	GO:0043226	organelle	0
Cellular component	GO:0043227	membrane-bounded organelle	0
Cellular component	GO:0005737	cytoplasm	0
Molecular function	GO:0003824	catalytic activity	0
Cellular component	GO:0005739	mitochondrion	0.01

Table S21. Gene Ontology and KEGG analysis in GOfuncR for genes with eQTL in European American in GENOA. Table lists the data source, GO term id, GO terms, and family wise error rate (FWER).

Ontology	Node id	Node name	FWER
Cellular component	GO:0005622	intracellular	0.01
Molecular function	GO:0003824	catalytic activity	0.01

Table S22. Gene Ontology and KEGG analysis in GOfuncR for genes without eQTL in African American in GENOA. Table lists the data source, GO term id, GO terms, and family wise error rate (FWER). (The table for European American is not shown here due to no significant term in the result.)

Ontology	Node id	Node name	FWER
Biological process	GO:0032501	multicellular organismal process	0
Biological process	GO:0007186	G protein-coupled receptor signaling pathway	0.01

Table S23. Number of genes in YRI GEUVADIS that are predicted above different R^2 thresholds using the gene expression prediction models constructed from GENOA or MESA. The gene expression prediction models are constructed based on GENOA (AA or EA) and MESA (AFA, CAU, or HIS).

	$R^2 \geq 0$	$R^2 \geq 0.01$	$R^2 \geq 0.02$	$R^2 \geq 0.05$	$R^2 \geq 0.1$	$R^2 \geq 0.2$	$R^2 \geq 0.5$
AAbslmm	2524	1581	1244	695	357	126	11
EAbslmm	2524	1355	985	488	202	67	6
AAelnet	2524	1513	1171	655	337	123	14
EAelnet	2524	1260	902	442	193	62	3
AFAelnet	2524	1310	904	433	192	69	8
CAUelnet	2524	1242	875	410	171	55	8
HISelnet	2524	1235	851	384	163	56	11

Table S24. Number of genes in GBR GEUVADIS that are predicted above different R^2 thresholds using the gene expression prediction models constructed from GENOA or MESA. The gene expression prediction models are constructed based on GENOA (AA or EA) and MESA (AFA, CAU, or HIS).

	$R^2 \geq 0$	$R^2 \geq 0.01$	$R^2 \geq 0.02$	$R^2 \geq 0.05$	$R^2 \geq 0.1$	$R^2 \geq 0.2$	$R^2 \geq 0.5$
AAbslmm	2524	1565	1238	774	443	193	25
EAbslmm	2524	1612	1302	820	457	200	20
AAelnet	2524	1508	1189	750	427	193	26
EAelnet	2524	1521	1213	739	415	191	21
AFAelnet	2524	1352	977	508	263	113	21
CAUelnet	2524	1417	1047	618	319	144	24
HISelnet	2524	1400	1037	593	308	135	26

Table S25. Number of genes in TSI GEUVADIS that are predicted above different R^2 thresholds using the gene expression prediction models constructed from GENOA or MESA. The gene expression prediction models are constructed based on GENOA (AA or EA) and MESA (AFA, CAU, or HIS).

	$R^2 \geq 0$	$R^2 \geq 0.01$	$R^2 \geq 0.02$	$R^2 \geq 0.05$	$R^2 \geq 0.1$	$R^2 \geq 0.2$	$R^2 \geq 0.5$
AAbslmm	2524	1561	1237	740	379	168	27
EAbslmm	2524	1622	1269	752	412	158	25
AAelnet	2524	1532	1193	703	366	166	24
EAelnet	2524	1539	1174	682	369	155	25
AFAelnet	2524	1300	901	449	248	107	18
CAUelnet	2524	1366	1017	560	298	128	21
HISelnet	2524	1359	982	531	287	120	21

Table S26. Number of genes in FIN GEUVADIS that are predicted above different R^2 thresholds using the gene expression prediction models constructed from GENOA or

MESA. The gene expression prediction models are constructed based on GENOA (AA or EA) and MESA (AFA, CAU, or HIS).

	$R^2 \geq 0$	$R^2 \geq 0.01$	$R^2 \geq 0.02$	$R^2 \geq 0.05$	$R^2 \geq 0.1$	$R^2 \geq 0.2$	$R^2 \geq 0.5$
AAbslmm	2524	1581	1276	776	408	177	28
EAbslmm	2524	1612	1289	791	438	184	25
AAelnet	2524	1528	1193	711	389	178	26
EAelnet	2524	1549	1196	708	412	170	23
AFAelnet	2524	1297	934	465	243	103	21
CAUelnet	2524	1413	1040	593	300	131	24
HISelnet	2524	1360	1016	555	292	120	26

Table S27. Number of genes in CEU GEUVADIS that are predicted above different R^2 thresholds using the gene expression prediction models constructed from GENOA or MESA. The gene expression prediction models are constructed based on GENOA (AA or EA) and MESA (AFA, CAU, or HIS).

	$R^2 \geq 0$	$R^2 \geq 0.01$	$R^2 \geq 0.02$	$R^2 \geq 0.05$	$R^2 \geq 0.1$	$R^2 \geq 0.2$	$R^2 \geq 0.5$
AAbslmm	2524	1476	1149	637	324	126	13
EAbslmm	2524	1550	1214	695	328	133	14
AAelnet	2524	1424	1106	618	299	124	15
EAelnet	2524	1433	1099	596	285	125	12
AFAelnet	2524	1256	866	415	213	93	9
CAUelnet	2524	1341	999	536	238	100	13
HISelnet	2524	1334	978	503	245	104	13

Table S28. Comparison of five different populations in the WTCCC data.

	AA		EA		AFA	CAU	HIS
	BSLMM	elnet	BSLMM	elnet	elnet	elnet	elnet
T1D	62(53)	30(24)	68(57)	24(18)	24(21)	31(27)	28(23)
T2D	0	0	1(1)	0	0	0	0
RA	18(18)	12(12)	24(24)	11(11)	13(13)	15(15)	14(14)
HT	0	0	0	0	0	0	0
CD	8(8)	5(5)	5(5)	1(1)	2(2)	0	1(1)
CAD	0	0	1(1)	0	0	0	0
BD	0	1(1)	0	0	1(1)	0	0
Total	88(79)	48(42)	99(88)	36(30)	40(37)	46(42)	43(38)

The table lists the number of genes passing the genome-wide significance threshold via Bonferroni correction ($\alpha = 0.05/\text{number of genes tested}$) in each of the seven common diseases. The numbers in the bracket are number of genes within 100kb of previously identified genes to be associated to the corresponding trait downloaded from GeneCards.

Table S29. Significant genes identified by GENOA AA (BSLMM) for different diseases in the WTCCC study. The table also lists the disease name, gene id, gene symbol, association strength (p value), gene position (chromosome number, transcription start site (TSS), transcription end site (TES)), and references that support the identified association. The diseases include Crohn's disease (CD), rheumatoid arthritis (RA), bipolar disorder (BD), type 1 diabetes (T1D), type 2 diabetes (T2D), coronary artery disease (CAD), and hypertension (HT). H indicates Human leukocyte antigen (HLA) region genes on chromosome 6, M indicates major histocompatibility complex (MHC) region, G indicates genes previously identified to be associated with diseases with supporting references, V indicates the vicinity of a reported gene.

Traits	GENE	Gene symbol	P value	Chromosome	TSS	TES	Reference
T1D	ENSG00000204389	HSPA1A	3.80E-85	6	31783291	31785723	¹ G,M,H
T1D	ENSG00000196735	HLA-DQA1	1.89E-79	6	32595956	32614839	¹ G,M,H
T1D	ENSG00000179344	HLA-DQB1	7.61E-47	6	32627244	32636160	¹ G,M,H
T1D	ENSG00000204516	MICB	8.07E-34	6	31462658	31478901	² G,M,H
T1D	ENSG00000241106	HLA-DOB	3.91E-33	6	32780540	32784825	¹ G,M,H
T1D	ENSG00000204290	BTNL2	2.73E-32	6	32359241	32379511	³ G,M,H
T1D	ENSG00000204511	MCCD1	1.57E-30	6	31496494	31498009	⁴ G,M,H
T1D	ENSG00000204428	LY6G5C	3.17E-27	6	31644461	31651817	⁴ H,M
T1D	ENSG00000204444	APOM	4.36E-27	6	31620193	31625987	⁵ G,M,H
T1D	ENSG00000213760	ATP6V1G2	5.41E-27	6	31512239	31516204	⁴ G, H,M
T1D	ENSG00000204421	LY6G6C	6.99E-25	6	31686425	31689622	⁴ G, H,M
T1D	ENSG00000243649	CFB	1.75E-24	6	31895475	31919861	⁴ G, H,M
T1D	ENSG00000204296	C6orf10	5.67E-24	6	32256303	32352332	⁴ G, H,M
T1D	ENSG00000204366	ZBTB12	9.57E-24	6	31867384	31869769	⁴ G, H,M
T1D	ENSG00000204301	NOTCH4	5.98E-21	6	32162620	32191844	⁴ G, H,M
T1D	ENSG00000204344	STK19	4.44E-20	6	31938868	31949228	⁴ G, H,M
T1D	ENSG00000204394	VAR5	5.97E-20	6	31745295	31763730	⁴ G, H,M
T1D	ENSG00000204386	NEU1	1.34E-17	6	31825436	31830683	⁴ G, H,M
T1D	ENSG00000204308	RNF5	1.11E-16	6	32146131	32151930	⁴ G, H,M
T1D	ENSG00000204435	CSNK2B	1.45E-16	6	31633013	31638120	¹ H,M
T1D	ENSG00000204472	AIF1	1.56E-15	6	31582961	31584798	⁴ G, H,M
T1D	ENSG00000204315	FKBP1	3.32E-15	6	32096484	32098068	⁶ H,M
T1D	ENSG00000204390	HSPA1L	1.02E-14	6	31777396	31783437	⁴ G, H,M
T1D	ENSG00000213676	ATF6B	1.34E-14	6	32065907	32096030	⁴ G, H,M
T1D	ENSG00000227507	LTB	1.75E-14	6	31548302	31550299	⁷ G,H,M
T1D	ENSG00000204388	HSPA1B	2.17E-14	6	31795512	31798031	⁴ G, H,M
T1D	ENSG00000204420	C6orf25	4.57E-14	6	31686371	31694491	⁸ H,M
T1D	ENSG00000213719	CLIC1	5.08E-14	6	31698358	31707540	⁸ H,M
T1D	ENSG00000204371	EHMT2	7.17E-14	6	31847536	31865464	⁴ G, H,M
T1D	ENSG00000204314	PRRT1	1.15E-12	6	32116136	32122150	⁴ G, H,M
T1D	ENSG00000232810	TNF	1.72E-12	6	31543344	31546113	⁸ G,H,M
T1D	ENSG00000204356	RDBP	2.67E-12	6	31919864	31926887	⁸ G,H,M
T1D	ENSG00000235863	B3GALT4	3.57E-12	6	33244917	33246602	⁹ G,M
T1D	ENSG00000226979	LTA	6.40E-12	6	31539831	31542101	⁸ G,H,M
T1D	ENSG00000227057	WDR46	8.42E-12	6	33246885	33257304	¹⁰ G,M
T1D	ENSG00000204209	DAXX	1.36E-11	6	33286335	33297046	¹⁰ M
T1D	ENSG00000204574	ABCF1	2.08E-11	6	30539153	30564956	¹⁰ G,H,M
T1D	ENSG00000231925	TAPBP	2.17E-11	6	33267471	33282164	¹⁰ G,M
T1D	ENSG00000234127	TRIM26	2.56E-11	6	30152232	30181204	¹¹ G,H
T1D	ENSG00000204520	MICA	3.00E-11	6	31367561	31384016	¹¹ G,H
T1D	ENSG00000237441	RLG2	8.71E-11	6	33259431	33267176	¹² M
T1D	ENSG00000204392	LSM2	1.70E-10	6	31765173	31774761	¹⁰ G,H,M
T1D	ENSG00000204264	PSMB8	3.49E-10	6	32808494	32812480	¹⁰ G,M,H
T1D	ENSG00000204228	HSD17B8	9.95E-10	6	33172419	33174608	¹³ G,M
T1D	ENSG00000236104	ZBTB22	1.07E-09	6	33282183	33285719	¹⁴ V,M
T1D	ENSG00000204310	AGPAT1	1.75E-09	6	32135989	32145873	¹⁰ G,M,H
T1D	ENSG00000204385	SLC44A4	2.52E-09	6	31830969	31846823	¹⁰ G,M,H
T1D	ENSG00000137411	VAR52	2.59E-09	6	30876019	30894236	¹⁵ V,M,H
T1D	ENSG00000204482	LST1	3.10E-09	6	31553901	31556686	¹⁰ G,M,H
T1D	ENSG00000197279	ZNF165	1.93E-08	6	28048753	28057341	¹⁶ G,M
T1D	ENSG00000204538	PSORS1C2	3.16E-08	6	31105313	31107127	⁴ G,M,H

T1D	ENSG00000223865	HLA-DPB1	1.11E-07	6	33043703	33054978	¹⁷ G,H,M
T1D	ENSG00000240053	LY6G5B	2.06E-07	6	31637944	31641553	¹⁰ G,M,H
T1D	ENSG00000204252	HLA-DOA	2.50E-07	6	32971955	32977389	¹ G,M,H
T1D	ENSG00000118655	DCLRE1B	3.86E-07	1	114447763	114456708	¹ G
T1D	ENSG00000111275	ALDH2	6.22E-07	12	112204691	112247782	¹⁸ V
T1D	ENSG00000089022	MAPKAPK5	1.03E-06	12	112279782	112334343	¹⁹ V
T1D	ENSG00000139531	SUOX	1.34E-06	12	56390964	56400425	¹ G
T1D	ENSG00000204438	GPANK1	1.60E-06	6	31629006	31634060	²⁰ V,M,H
T1D	ENSG00000204610	TRIM15	2.32E-06	6	30130983	30140473	¹⁰ G,M,H
T1D	ENSG00000137331	IER3	2.47E-06	6	30710976	30712331	¹⁰ G,M,H
T1D	ENSG00000204700	OR2J2	2.51E-06	6	29141311	29142351	²¹ V,M
RA	ENSG00000243649	CFB	1.72E-14	6	31895475	31919861	²² V,M,H
RA	ENSG00000196735	HLA-DQA1	1.98E-14	6	32595956	32614839	²³ G,M,H
RA	ENSG00000204348	DOM3Z	1.02E-13	6	31937587	31940069	²⁴ G,M,H
RA	ENSG00000204366	ZBTB12	4.04E-12	6	31867384	31869769	²⁵ V,M,H
RA	ENSG00000204610	TRIM15	1.17E-11	6	30130983	30140473	²⁶ V,M,H
RA	ENSG00000204371	EHMT2	1.04E-10	6	31847536	31865464	²⁷ G,M,H
RA	ENSG00000204304	PBX2	1.46E-09	6	32151966	32157963	²⁸ G,M,H
RA	ENSG00000179344	HLA-DQB1	1.73E-09	6	32627244	32636160	²⁹ G,M,H
RA	ENSG00000258388	XXbac-BPG300A18.12	4.92E-09	6	32121622	32139755	³⁰ V,M,H
RA	ENSG00000198502	HLA-DRB5	1.01E-08	6	32485120	32498064	³¹ G,M,H
RA	ENSG00000237441	RGL2	1.17E-08	6	33259431	33267176	³² G,M
RA	ENSG00000196126	HLA-DRB1	1.51E-08	6	32546546	32557625	³³ G,M,H
RA	ENSG00000204315	FKBPL	2.39E-08	6	32096484	32098068	³⁴ G,M,H
RA	ENSG00000231852	CYP21A2	1.56E-07	6	32006042	32009447	³⁵ V,M,H
RA	ENSG00000234745	HLA-B	2.90E-07	6	31321649	31324965	³⁶ G,M,H
RA	ENSG00000204209	DAXX	3.24E-07	6	33286335	33297046	³⁷ G,M
RA	ENSG00000232629	HLA-DQB2	3.39E-07	6	32723875	32731311	³⁶ G,M,H
RA	ENSG00000241106	HLA-DOB	3.80E-07	6	32780540	32784825	³⁶ G,M,H
CD	ENSG00000162594	IL23R	1.15E-13	1	67632083	67725662	³⁸ G
CD	ENSG00000140807	NKD1	1.16E-09	16	50582241	50670647	¹⁶ V
CD	ENSG00000167208	SNX20	1.30E-08	16	50700211	50715264	³⁹ V
CD	ENSG00000119919	NKX2-3	5.20E-08	10	101292690	101296278	⁴⁰ V
CD	ENSG00000237693	IRGM	2.14E-07	5	150226085	150280298	⁴¹ V
CD	ENSG00000120053	GOT1	8.50E-07	10	101156627	101190393	⁴² V
CD	ENSG00000164062	APEH	1.12E-06	3	49711435	49721396	⁴³ V
CD	ENSG00000256235	C5orf62	1.24E-06	5	150157508	150176296	⁴⁴ V

Reference

1. Brorsson, C., Tue Hansen, N., Bergholdt, R., Brunak, S., and Pociot, F. (2010). The type 1 diabetes - HLA susceptibility interactome--identification of HLA genotype-specific disease genes for type 1 diabetes. *PLoS One* 5, e9576.
2. Field, S.F., Nejentsev, S., Walker, N.M., Howson, J.M., Godfrey, L.M., Jolley, J.D., Hardy, M.P., and Todd, J.A. (2008). Sequencing-based genotyping and association analysis of the MICA and MICB genes in type 1 diabetes. *Diabetes* 57, 1753-1756.
3. Orozco, G., Eerligh, P., Sanchez, E., Zhernakova, S., Roep, B.O., Gonzalez-Gay, M.A., Lopez-Nevot, M.A., Callejas, J.L., Hidalgo, C., Pascual-Salcedo, D., et al. (2005). Analysis of a functional BTNL2 polymorphism in type 1 diabetes, rheumatoid arthritis, and systemic lupus erythematosus. *Hum Immunol* 66, 1235-1241.
4. Santiago, J.L., Li, W., Lee, A., Martinez, A., Chandrasekaran, A., Fernandez-Arquero, M., Khalili, H., de la Concha, E.G., Urcelay, E., and Gregersen, P.K. (2009). Localization of Type 1 Diabetes susceptibility in the ancestral haplotype 18.2 by high density SNP mapping. *Genomics* 94, 228-232.
5. Frej, C., Mendez, A.J., Ruiz, M., Castillo, M., Hughes, T.A., Dahlback, B., and Goldberg, R.B. (2017). A Shift in ApoM/S1P Between HDL-Particles in Women With Type 1 Diabetes Mellitus Is Associated With Impaired Anti-Inflammatory Effects of the ApoM/S1P Complex. *Arterioscl Throm Vas* 37, 1194-1205.
6. Cipriani, V., Leung, H.T., Plagnol, V., Bunce, C., Khan, J.C., Shahid, H., Moore, A.T., Harding, S.P., Bishop, P.N., Hayward, C., et al. (2012). Genome-wide association study of age-related macular degeneration identifies associated variants in the TNXB-FKBPL-NOTCH4 region of chromosome 6p21.3. *Hum Mol Genet* 21, 4138-4150.
7. Ramalho, T., Filgueiras, L., Silva, I.A., Pessoa, A.F.M., and Jancar, S. (2018). Impaired wound healing in type 1 diabetes is dependent on 5-lipoxygenase products. *Sci Rep-Uk* 8.
8. Valdes, A.M., Thomson, G., and Consortium, T.D.G. (2009). Several loci in the HLA class III region are associated with T1D risk after adjusting for DRB1-DQB1. *Diabetes Obes Metab* 11, 46-52.
9. Holm, L.J., Krogvold, L., Hasselby, J.P., Kaur, S., Claessens, L.A., Russell, M.A., Mathews, C.E., Hanssen, K.F., Morgan, N.G., Koeleman, B.P.C., et al. (2018). Abnormal islet sphingolipid metabolism in type 1 diabetes. *Diabetologia* 61, 1650-1661.
10. Shiina, T., Hosomichi, K., Inoko, H., and Kulski, J.K. (2009). The HLA genomic loci map: expression, interaction, diversity and disease. *J Hum Genet* 54, 15-39.
11. Nyaga, D.M., Vickers, M.H., Jefferies, C., Perry, J.K., and O'Sullivan, J.M. (2018). Type 1 Diabetes Mellitus-Associated Genetic Variants Contribute to Overlapping Immune Regulatory Networks. *Front Genet* 9, 535.
12. Herberg, J.A., Beck, S., and Trowsdale, J. (1998). TAPASIN, DAXX, RGL2, HKE2 and four new genes (BING 1, 3 to 5) form a dense cluster at the centromeric end of the MHC. *J Mol Biol* 277, 839-857.
13. Kawabata, Y., Ikegami, H., Awata, T., Imagawa, A., Maruyama, T., Kawasaki, E., Tanaka, S., Shimada, A., Osawa, H., Kobayashi, T., et al. (2009). Differential association of HLA with three subtypes of type 1 diabetes: fulminant, slowly progressive and acute-onset. *Diabetologia* 52, 2513-2521.
14. Larsen, C.E., Alford, D.R., Trautwein, M.R., Jalloh, Y.K., Tarnacki, J.L., Kunnenkeri, S.K., Fici, D.A., Yunis, E.J., Awdeh, Z.L., and Alper, C.A. (2014). Dominant sequences of

- human major histocompatibility complex conserved extended haplotypes from HLA-DQA2 to DAXX. *PLoS Genet* 10, e1004637.
15. Orru, V., Steri, M., Sole, G., Sidore, C., Virdis, F., Dei, M., Lai, S., Zoledziwska, M., Busonero, F., Mulas, A., et al. (2013). Genetic variants regulating immune cell levels in health and disease. *Cell* 155, 242-256.
 16. Gamazon, E.R., Wheeler, H.E., Shah, K.P., Mozaffari, S.V., Aquino-Michaels, K., Carroll, R.J., Eyler, A.E., Denny, J.C., Nicolae, D.L., Cox, N.J., et al. (2015). A gene-based association method for mapping traits using reference transcriptome data. *Nat Genet* 47, 1091-1098.
 17. Noble, J.A., and Valdes, A.M. (2011). Genetics of the HLA region in the prediction of type 1 diabetes. *Curr Diab Rep* 11, 533-542.
 18. Pan, G., Deshpande, M., Thandavarayan, R.A., and Palaniyandi, S.S. (2016). ALDH2 Inhibition Potentiates High Glucose Stress-Induced Injury in Cultured Cardiomyocytes. *J Diabetes Res* 2016, 1390861.
 19. Kaldunski, M., Jia, S., Geoffrey, R., Basken, J., Prosser, S., Kansra, S., Mordes, J.P., Lernmark, A., Wang, X., and Hessner, M.J. (2010). Identification of a serum-induced transcriptional signature associated with type 1 diabetes in the BioBreeding rat. *Diabetes* 59, 2375-2385.
 20. Goudey, B., Abraham, G., Kikianty, E., Wang, Q., Rawlinson, D., Shi, F., Haviv, I., Stern, L., Kowalczyk, A., and Inouye, M. (2017). Interactions within the MHC contribute to the genetic architecture of celiac disease. *Plos One* 12, e0172826.
 21. Yucesoy, B., Talzhanov, Y., Johnson, V.J., Wilson, N.W., Biagini, R.E., Wang, W., Frye, B., Weissman, D.N., Germolec, D.R., Luster, M.I., et al. (2013). Genetic variants within the MHC region are associated with immune responsiveness to childhood vaccinations. *Vaccine* 31, 5381-5391.
 22. Juyal, G., Negi, S., Sood, A., Gupta, A., Prasad, P., Senapati, S., Zaneveld, J., Singh, S., Midha, V., van Sommeren, S., et al. (2015). Genome-wide association scan in north Indians reveals three novel HLA-independent risk loci for ulcerative colitis. *Gut* 64, 571-579.
 23. Hao, G.F., Li, Y.S., Liu, J.L., and Wo, M.Y. (2014). Association of HLA-DQA1 (rs9272219) with susceptibility to rheumatoid arthritis in a Han Chinese population. *Int J Clin Exp Pathol* 7, 8155-8158.
 24. Tamiya, G., Shinya, M., Imanishi, T., Ikuta, T., Makino, S., Okamoto, K., Furugaki, K., Matsumoto, T., Mano, S., Ando, S., et al. (2005). Whole genome association study of rheumatoid arthritis using 27 039 microsatellites. *Human Molecular Genetics* 14, 2305-2321.
 25. Emilsson, V., Ilkov, M., Lamb, J.R., Finkel, N., Gudmundsson, E.F., Pitts, R., Hoover, H., Gudmundsdottir, V., Horman, S.R., Aspelund, T., et al. (2018). Co-regulatory networks of human serum proteins link genetics to disease. *Science* 361, 769-773.
 26. Venkateswaran, S., Prince, J., Cutler, D.J., Marigorta, U.M., Okou, D.T., Prahalad, S., Mack, D., Boyle, B., Walters, T., Griffiths, A., et al. (2018). Enhanced Contribution of HLA in Pediatric Onset Ulcerative Colitis. *Inflamm Bowel Dis* 24, 829-838.
 27. Renauer, P.A., Saruhan-Direskeneli, G., Coit, P., Adler, A., Aksu, K., Keser, G., Alibaz-Oner, F., Aydin, S.Z., Kamali, S., Inanc, M., et al. (2015). Identification of Susceptibility Loci in IL6, RPS9/LILRB3, and an Intergenic Locus on Chromosome 21q22 in Takayasu Arteritis in a Genome-Wide Association Study. *Arthritis Rheumatol* 67, 1361-1368.

28. van Steenbergen, H.W., Luijk, R., Shoemaker, R., Heijmans, B.T., Huizinga, T.W.J., and van der Helm-van Mil, A.H.M. (2014). Differential methylation within the major histocompatibility complex region in rheumatoid arthritis: a replication study. *Rheumatology* 53, 2317-2318.
29. Wu, J., Li, J., Li, S., Zhang, T.P., Li, L.J., Lv, T.T., Pan, H.F., and Ye, D.Q. (2017). Association of HLA-DQB1 polymorphisms with rheumatoid arthritis: a meta-analysis. *Postgrad Med J* 93, 618-625.
30. Yau, A.C., Tuncel, J., Haag, S., Norin, U., Houtman, M., Padyukov, L., and Holmdahl, R. (2016). Conserved 33-kb haplotype in the MHC class III region regulates chronic arthritis. *Proc Natl Acad Sci U S A* 113, E3716-3724.
31. Kim, K., Bang, S.Y., Yoo, D.H., Cho, S.K., Choi, C.B., Sung, Y.K., Kim, T.H., Jun, J.B., Kang, Y.M., Suh, C.H., et al. (2016). Imputing Variants in HLA-DR Beta Genes Reveals That HLA-DRB1 Is Solely Associated with Rheumatoid Arthritis and Systemic Lupus Erythematosus. *Plos One* 11, e0150283.
32. Edwards, C.J., Feldman, J.L., Beech, J., Shields, K.M., Stover, J.A., Trepicchio, W.L., Larsen, G., Foxwell, B.M., Brennan, F.M., Feldmann, M., et al. (2007). Molecular profile of peripheral blood mononuclear cells from patients with rheumatoid arthritis. *Mol Med* 13, 40-58.
33. Kerlan-Candon, S., Combe, B., Vincent, R., Clot, J., Pinet, V., and Eliaou, J.F. (2001). HLA-DRB1 gene transcripts in rheumatoid arthritis. *Clin Exp Immunol* 124, 142-149.
34. Huffman, K.M., Jessee, R., Andonian, B., Davis, B.N., Narowski, R., Huebner, J.L., Kraus, V.B., McCracken, J., Gilmore, B.F., Tune, K.N., et al. (2017). Molecular alterations in skeletal muscle in rheumatoid arthritis are related to disease activity, physical inactivity, and disability. *Arthritis Res Ther* 19, 12.
35. Falhammar, H., Frisen, L., Hirschberg, A.L., Nordenskjold, A., Almqvist, C., and Nordenstrom, A. (2019). Increased Risk of Autoimmune Disorders in 21-Hydroxylase Deficiency: A Swedish Population-Based National Cohort Study. *J Endocr Soc* 3, 1039-1052.
36. van Drongelen, V., and Holoshitz, J. (2017). A reciprocal HLA-disease association in rheumatoid arthritis and pemphigus vulgaris. *Front Biosci-Landmark* 22, 909-919.
37. Meinecke, I., Cinski, A., Baier, A., Peters, M.A., Dankbar, B., Wille, A., Drynda, A., Mendoza, H., Gay, R.E., Hay, R.T., et al. (2007). Modification of nuclear PML protein by SUMO-1 regulates Fas-induced apoptosis in rheumatoid arthritis synovial fibroblasts. *Proc Natl Acad Sci U S A* 104, 5073-5078.
38. Chang, M., Saiki, R.K., Cantanese, J.J., Lew, D., van der Helm-van Mil, A.H., Toes, R.E., Huizinga, T.W., Ardlie, K.G., Criswell, L.A., Seldin, M.F., et al. (2008). The inflammatory disease-associated variants in IL12B and IL23R are not associated with rheumatoid arthritis. *Arthritis Rheum* 58, 1877-1881.
39. Peters, J.E., Lyons, P.A., Lee, J.C., Richard, A.C., Fortune, M.D., Newcombe, P.J., Richardson, S., and Smith, K.G.C. (2016). Insight into Genotype-Phenotype Associations through eQTL Mapping in Multiple Cell Types in Health and Immune-Mediated Disease. *Plos Genetics* 12, e1005908.
40. McGovern, D.P., Gardet, A., Torkvist, L., Goyette, P., Essers, J., Taylor, K.D., Neale, B.M., Ong, R.T., Lagace, C., Li, C., et al. (2010). Genome-wide association identifies multiple ulcerative colitis susceptibility loci. *Nat Genet* 42, 332-337.

41. de Lange, K.M., Moutsianas, L., Lee, J.C., Lamb, C.A., Luo, Y., Kennedy, N.A., Jostins, L., Rice, D.L., Gutierrez-Achury, J., Ji, S.G., et al. (2017). Genome-wide association study implicates immune activation of multiple integrin genes in inflammatory bowel disease. *Nat Genet* 49, 256-261.
42. Kulecka, M., Wierzbicka, A., Paziewska, A., Mikula, M., Habor, A., Janczyk, W., Dabrowska, M., Karczmariski, J., Lazniewski, M., Ginalski, K., et al. (2017). A heterozygous mutation in GOT1 is associated with familial macro-aspartate aminotransferase. *J Hepatol* 67, 1026-1030.
43. Anderson, C.A., Boucher, G., Lees, C.W., Franke, A., D'Amato, M., Taylor, K.D., Lee, J.C., Goyette, P., Imielinski, M., Latiano, A., et al. (2011). Meta-analysis identifies 29 additional ulcerative colitis risk loci, increasing the number of confirmed associations to 47. *Nat Genet* 43, 246-252.
44. Wellcome Trust Case Control, C., Craddock, N., Hurles, M.E., Cardin, N., Pearson, R.D., Plagnol, V., Robson, S., Vukcevic, D., Barnes, C., Conrad, D.F., et al. (2010). Genome-wide association study of CNVs in 16,000 cases of eight common diseases and 3,000 shared controls. *Nature* 464, 713-720.